TOPICAL REVIEW

A review of gallium oxide-based power Schottky barrier diodes

To cite this article: Xueqiang Ji *et al* 2022 *J. Phys. D: Appl. Phys.* **55** 443002

IOP Publishing Journal of Physics D: Applied Physics
J. Phys. D: Appl. Phys. **55** (2022) 443002 (20pp) https://doi.org/10.1088/1361-6463/ac855c

Topical Review

A review of gallium oxide-based power Schottky barrier diodes

Xueqiang Ji[1], Chao Lu[1], Zuyong Yan[1], Li Shan[2], Xu Yan[1], Jinjin Wang[1], Jianying Yue[1], Xiaohui Qi[1], Zeng Liu[2,3], Weihua Tang[2,3,*] and Peigang Li[1,*]

[1] School of Integrated Circuits & State Key Laboratory of Information Photonics and Optical Communications, Beijing University of Posts and Telecommunications, Beijing 100876, People's Republic of China
[2] College of Integrated Circuit Science and Engineering, Nanjing University of Posts and Telecommunications, Nanjing 210023, People's Republic of China
[3] National and Local Joint Engineering Laboratory for RF Integration and Micro-Packing Technologies, Nanjing University of Posts and Telecommunications, Nanjing 210023, People's Republic of China

E-mail: whtang@njupt.edu.cn and pgli@bupt.edu.cn

Received 16 March 2022, revised 17 July 2022
Accepted for publication 29 July 2022
Published 8 September 2022

Abstract

Gallium oxide (Ga_2O_3) is a representative of ultra-wide bandgap semiconductors, with a band gap of about 4.9 eV. In addition to a large dielectric constant and excellent physical and chemical stability, Ga_2O_3 has a theoretical breakdown electric field strength of more than 8 MV cm^{-1}, which is 27 times more than that of Si and about twice as large as that of SiC and GaN. It is guaranteed that Ga_2O_3 has irreplaceable applications in ultra-high-power (1–10 kW) electronic devices. Unfortunately, due to the difficulty of p-type doping of Ga_2O_3, the full Ga_2O_3-based bipolar devices face more difficulties, and the unipolar Ga_2O_3 power Schottky diodes are feasible, but substantial progress has been made in recent years. In this article, we review the advanced progress and important achievements of the state-of-the-art Ga_2O_3-based power Schottky barrier diodes, and provide staged guidance for the further development of Ga_2O_3 power devices. Multiple types of device architectures, including basic structure, edge terminal processing, field-plated, trench and heterojunction p–n structure, will be discussed in detail.

Keywords: gallium oxide (Ga_2O_3), Schottky barrier diodes (SBDs), power devices

(Some figures may appear in colour only in the online journal)

1. Introduction

Power electronic devices will play an important role in future high-power, high-voltage applications, which can hardly be achieved by traditional silicon devices [1–4]. In particular, there will be very broad prospects for the development of electric automobiles, 5G, Internet of Things and in emerging application fields in the future. Si-based power devices, as the most mature power conversion chips, have reached their maximum capacity for power transmission, which means that they are unlikely to be the preferred choice for the next-generation higher-power devices due to increasing uneconomic R&D. As a result, wide-bandgap semiconductor-based power devices, mainly silicon carbide (SiC) and gallium nitride (GaN)-based devices have developed rapidly [5, 6]. As a representative of the third-generation semiconductors, SiC and GaN have very high breakdown voltage and low on-resistance that make them

* Authors to whom any correspondence should be addressed.

the ideal choices for high-power devices, making up for (even replacing) the commercial layout of Si-based power electronic devices [7–10].

Gallium oxide (Ga_2O_3) is a semiconductor material with a band gap of about 4.3–4.9 eV, varying in its five different phases (α, β, γ, δ and ε), which is larger than that of SiC (3.3 eV) and GaN (3.4 eV) [11–13]. The critical theoretical electric field strength of Ga_2O_3 is up to 8 MV cm^{-1}, which is 27 times more than that of Si, three times greater than that of SiC, and twice as much as that of GaN [14–17]. It is guaranteed to have great potential for applications in ultra-high-voltage electronic devices. Baliga's figure of merit (BFOM), a key parameter to evaluate the suitability of power device fabrications, of Ga_2O_3 (>3000) is much larger than that of SiC and GaN by ten and four times, respectively, indicating that Ga_2O_3 is one of the most promising candidates for next-generation power electronics. Current edge-defined film-fed growth (EFG) technologies of β-Ga_2O_3 crystal have the advantage of low-cost, larger size and good crystal quality. High-quality epitaxial films of different thicknesses can be easily grown by metal-organic chemical vapor deposition (MOCVD), HVPE, molecular beam epitaxy (MBE), etc [18–26]. In addition, the substrate and epitaxy of Ga_2O_3 have easily tunable n-type doping ranging from semi-insulating to conductive, which boosts the development of Ga_2O_3 power electronics devices [27–31].

Over the past few decades, although GaN and SiC power devices have gradually replaced Si-based power devices in many applications, the industrial pain point of large-scale and high-cost GaN and SiC substrates is the most critical challenge for achieving high-performance power devices [32–34]. The high-quality, large-size and low-cost Ga_2O_3 substrates enable more promising opportunities for the semiconductor power device market [35, 36]. Compared to traditional p–n junction diodes, Schottky barrier diodes (SBDs) have lower turn-on voltages and faster recovery times, which results in them being commonly used as high-voltage and high-speed switching devices [37, 38]. In recent years, continuous investment has promoted significant progress for Ga_2O_3 SBDs with material advantage and mature n-type doping. However, the absence of p-type Ga_2O_3 directly hinders the design of bipolar devices [39]. Therefore, when one needs to solve the p-type problem, the unipolar Ga_2O_3 SBDs are most likely to be mass-produced first. Since Ga_2O_3-SBD simply fabricated using single-crystal β-Ga_2O_3 (010) substrates was reported in 2013 [40], Ga_2O_3 SBDs have been developing towards high breakdown voltage (V_{BR}), low on-resistance (R_{ON}) and low production cost. In recent years, there has been a tremendous increase in research papers on Ga_2O_3 SBDs. By optimizing the epitaxial material, device structure and device fabrication process, there has been a continuous improvement in the performance of Ga_2O_3 SBDs. Ga_2O_3 SBDs have made a great breakthrough in high breakdown voltage, and some enterprises and research institutes have entered the stage of mass production. For example, Novel Crystal Technology Ltd has introduced an ampere-class 1200 V-Ga_2O_3 SBDs.

In this review, we summarize the current advances in technology and progress of Ga_2O_3-based SBDs. Specifically, a detailed introduction is carried out in various R&D teams who have reported mechanisms and methods, mainly including basic structure, field plate (FP), trench structure, ion implementation, thermal oxygen terminal and p-type heterojunction. The Ga_2O_3 substrate and epitaxy and material properties are discussed in section 2., Contacts between metal/Ga_2O_3 is introduced in section 3. Section 4 contains the current progress of Ga_2O_3 SBDs and heterojunction diodes (HJDs). Finally, the summary and prospects are covered in section 5.

2. Ga_2O_3 substrate and epitaxy

Ga_2O_3 is a transparent ultra-wide-bandgap oxide semiconductor material, which contains multiple-phase structures, all of which can be converted to β phase under certain conditions [12, 41–43]. Ga_2O_3 is the preferred semiconductor material for manufacturing high-temperature, high-frequency, high-power microelectronic devices and solar-blind UV photodetectors. In addition, compared to diamond, which is limited by its large size and high-quality single-crystal growth technology, Ga_2O_3 single crystal can be grown by economical and efficient melt preparation technologies, with high speed, low cost and high yield. Table 1 summarizes the relevant parameters of several common semiconductors, which demonstrates many material advantages of Ga_2O_3, such as wide band gap, high theoretical breakdown field strength (8 MV cm^{-1}) and large BFOM. These advantages make it an ideal material for power electronics, such as high-voltage rectifiers and enhancement-mode metal-oxide field-effect transistors. At present, the majority of the substrates used in Ga_2O_3 SBD, as reported in the literature, were purchased or supplied by Japanese NCT. High-quality 6 inch Ga_2O_3 single crystal was successfully grown by EFG, and the industrialization of 4 inch Ga_2O_3 single crystal is available, which is currently the leading position in the world [13, 16], as shown in figure 1.

As the drift and channel layer, the high-quality epitaxial layer is important for Ga_2O_3 film power devices. At present, the majority of Ga_2O_3 power devices have always been reported achieving high-quality homoepitaxy or heteroepitaxy Ga_2O_3 film using hydride vapor phase epitaxy (HVPE) [44, 45], MBE [46, 47], MOCVD [48, 49], pulsed laser deposition [50, 51], physical vapor deposition (PVD) [52, 53] and mist CVD [44, 54]. HVPE and MBE are two of the most popular epitaxial growth tools and are also available commercially. Recently, HVPE has been successfully applied to thick epitaxial layers in most Ga_2O_3 SBD devices, and MBE has been widely used in the preparation of high-quality thin-drift layer films in Ga_2O_3 metal-oxide-semiconductor field effect transistor (MOSFET) devices.

HVPE is one of the most promising approaches in terms of deposition rate, layer quality and inexpensive facility. However, HVPE-grown films always have a rough surface, which requires a post-chemical mechanical polishing process to smooth it. MBE has very low surface roughness, but its slow growth rate limits its further development. As a mature epitaxial growth technique that has been widely used in GaAs and GaN epitaxial growth, MOCVD possesses great potential in

Table 1. Comparison of the performance parameters of the main semiconductor materials.

Material	Si	GaAs	4H-SiC	GaN	Diamond	Ga_2O_3
Band gap (eV)	1.1	1.43	3.25	3.4	5.5	4.85
Electron mobility ($cm^2\ V^{-1}\ s^{-1}$)	1480	8400	1000	1250	2000	300
Dielectric constant	11.8	12.9	9.7	9	5.5	10
Baliga ($\varepsilon\mu E_b^3$)	1	14.7	317	846	24 660	3214
Breakdown field ($MV\ cm^{-1}$)	0.3	0.4	2.5	3.3	10	8

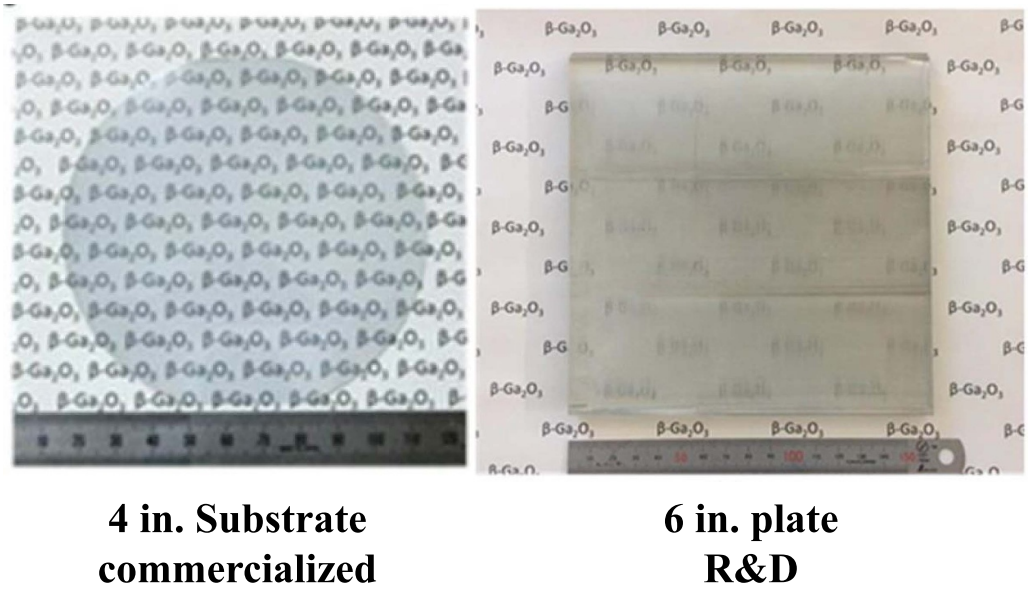

Figure 1. Status of EFG-grown bulk Ga_2O_3 wafer sizes. Reproduced from [16]. © IOP Publishing Ltd. CC BY 3.0.

commercial Ga_2O_3 epitaxial wafers in terms of fast deposition rate, smooth surface quality and mature growth process. The mist CVD technique is a safe, inexpensive and energy-saving method of film formation, without special components and a vacuum system. Mist-grown α-Ga_2O_3 films exhibit good crystal and surface roughness, which shows a high-performance α-Ga_2O_3 SBD device, with lower R_{ON} and greater V_{BR} compared to SiC-SBD. The multi-epitaxial technology development provides a good guarantee for Ga_2O_3 thin-film devices.

3. Contact between metal and Ga_2O_3

The basic structure of Ga_2O_3 SBDs is composed of Ga_2O_3 material and Schottky contacts for the anode and Ohmic contacts for the cathode. Furthermore, the contact between metal and Ga_2O_3 is the main determinant of electron transport between interfaces, which further affects the performance of the device. The Schottky barrier is an intrinsic property that affects the charge transport at the metal–semiconductor interface, first proposed by Mott and called Mott's theory [38]. The Schottky barrier is generally the difference between the electron affinity energy of a metal and that of a semiconductor. The Schottky barrier height (SBH) is expressed as,

$$\Phi_B = \Phi_m - \chi, \tag{1}$$

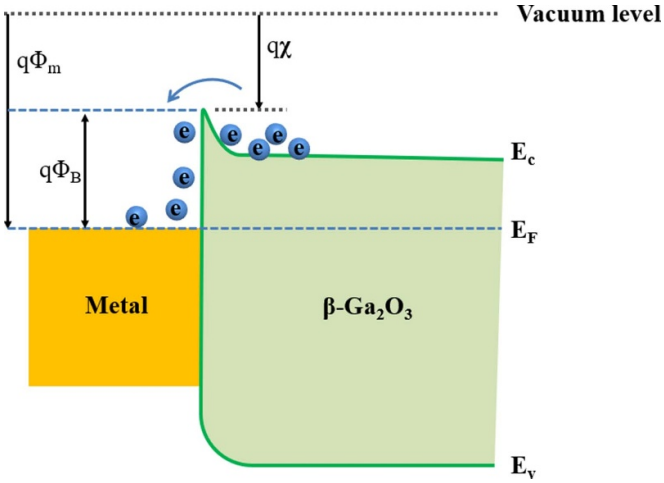

Figure 2. Schematic energy band diagrams of metal/Ga_2O_3 contact.

where Φ_m stands for the work function of the metal and χ is the electron affinity of the Ga_2O_3. The schematic energy band diagram of the formation of metal/Ga_2O_3 contact is shown in figure 2. When the metal and semiconductor contact, in order to make the Fermi energy level equal, the energy band of the Ga_2O_3 bends upwards and thus forms a large Schottky barrier at the Ga_2O_3/metal interface. The SBH is usually determined using experimental methods such as current–voltage (I–V) or

Table 2. Summary of Schottky contacts on Ga_2O_3.

Metal	Materials orientation (N cm^{-3})	SBH (eV)	n	References
Au	β-Ga_2O_3 (100) (10^{17}–10^{18})	1.2 (*I–V*)	1.1	[66]
Au	β-Ga_2O_3 (100) (6×10^{16}–8×10^{17})	1.23 (PES)	1.02–1.09	[67]
Au	α-Ga_2O_3 (0001) (2×10^{17}–7×10^{17})	1.7–2.0 (*I–V*)	1.1	[68]
Au	β-Ga_2O_3 (010) UID	1.97 (*C–V*)	1.09	[69]
Ni	β-Ga_2O_3 (010) UID	1.54 (*C–V*)	1.04	[69]
Ni	β-Ga_2O_3 (100) (6×10^{16}–8×10^{17})	0.97 (*I–V*) 1.22 (*C–V*)	—	[70]
Cu	β-Ga_2O_3 (−201) (5–8×10^{18})	1.13 ± 0.1 (*I–V*)	1.53 ± 0.2	[61]
Cu	β-Ga_2O_3 (−201) (1.6×10^{18})	0.8–0.95 (*I–V*)	1.2–1.4	[71]
Pt	β-Ga_2O_3 (010) UID	1.59 (*C–V*)	1.03	[69]
Pt	β-Ga_2O_3 (010) (3×10^{16}–5×10^{16})	1.3–1.5	∼1	[40]
Pt	β-Ga_2O_3 (001) (1×10^{16})	1.09–1.15	1.03 ± 0.01	[72]
Pt	β-Ga_2O_3 (100) (2.3×10^{14})	1.3–1.39 (*I–V*)	1.1	[73]
W	β-Ga_2O_3 (−201) (5–8×10^{18})	0.91 ± 0.09 (*I–V*)	1.40 ± 0.4	[61]
	β-Ga_2O_3 (010) UID	1.05 ± 0.03 (*I–V*)	2.68 ± 0.3	
W	β-Ga_2O_3 (−201) (2×10^{17})	0.97 (*I–V*)	1.04	[74]
Ir	β-Ga_2O_3 (−201) (5–8×10^{18})	1.29 ± 0.1 (*I–V*)	1.45 ± 0.2	[61]
	β-Ga_2O_3 (010) UID	1.40 ± 0.08 (*I–V*)	1.64 ± 0.2	
Mo	β-Ga_2O_3 (110) (2×10^{17})	1.55 (*I–V*)	—	[75]
Pd	β-Ga_2O_3 (010) UID	1.28 (*C–V*)	1.05	[69]

capacitance–voltage (*C–V*). Experimental results show that the SBH of some semiconductors is only weakly dependent on the metal work function but depends mainly on the intrinsic properties of the semiconductor, as well as on the interface structure and interactions [55]. Therefore, the research on metal–semiconductor (M–S) contacts is essential, and the choice of metal electrode metal is also an important aspect of constructing Ga_2O_3 SBD devices. In addition, the high-conductivity compounds used as electrodes, such as Ga_2O_3 and TiN, form stable interfaces with Ga_2O_3 and exhibit excellent electron transfer performance, [56]. This section briefly introduces the progress and content related to the contact between Ga_2O_3 and metal materials.

3.1. Ohmic contacts to Ga_2O_3

Usually, an excellent Ohmic contact has low or even no SBHs, and exhibits a linear current−voltage curve, which minimizes the energy consumption and also prevents thermal effects caused by contact resistance. This is especially important due to the intrinsic low thermal conductivity of Ga_2O_3. Hence, a superior Ga_2O_3 Ohmic contact is a prerequisite for achieving a high-performance device. Lee *et al* [57] described the interfacial reaction of Ti/Ga_2O_3 in detail and confirmed that Ti/Ga_2O_3 has a good Ohmic contact. Currently, most of the Ga_2O_3 device articles use Ti metal as the Ohmic contact [18, 37, 58–62]. Based on this, several effective methods have been used to further reduce the Ohmic contact resistance, such as doping [63], surface treatment [64], plasma treatment [65], etc. A recent report shows that Ga_2O_3 with heavy (n^+) Si-doped ($\sim 1.8 \times 10^{20}$ cm^{-3}) exhibits a record low Au/Ti/Ga_2O_3 (n^+) contact resistance of 80 mΩ mm with specific contact resistivity of 8.3×10^{-7} Ω cm^2 [63]. Jeong *et al* demonstrated Ohmic behavior with specific resistivity of 2.0×10^{-3} Ω cm^2 and contact resistance of 0.8 Ω m by using CF_4 plasma for surface treatment without any post-thermal annealing [64]. Massabuau *et al* reported the impact of annealing temperature on the Ohmic contact between Ti and α-Ga_2O_3 and demonstrated that 450 °C is optimal due to the fast diffusion channel provided at this temperature [65]. Therefore, Ti metal is the most promising and dominant Ohmic contact metal material for now.

3.2. Schottky contacts to Ga_2O_3

The Schottky diode is a majority-carrier-conducting device without the problem of minority carrier lifetime and reverse recovery, which is completely different to the reverse recovery of p–n junction diode caused by the recombination of electrons and holes. In addition, the SBH is lower than the p–n junction barrier. This advantage gives Schottky diodes a high switching frequency and a lower forward voltage.

In the early stage, most of the reports focused on the electronic properties of Ga_2O_3 SBD devices using metal−semiconductor Schottky contact structure without terminal design, surface passivation and other optimized processes. In this section, we briefly sum up the electronic behavior of Ga_2O_3 with various Schottky metals. There have been studies of Schottky contacts on different Ga_2O_3 orientation surfaces to analyze their characteristics, such as barrier height (SBH) and ideality factor (n). The characteristic performance of Schottky barriers is generally analyzed by *I–V*, CV curves. The details of different studies are summarized in table 2. The selection of a suitable Schottky metal electrode is a cornerstone for future studies of Ga_2O_3 Schottky SBD device performance. However, we are also aware that different interface characteristics and contact environments can affect the Schottky barrier, which requires specific analysis in each

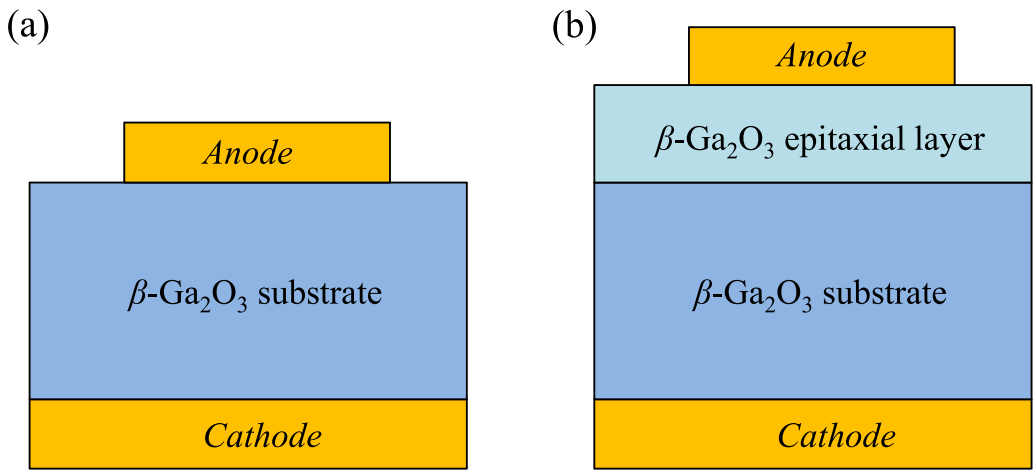

Figure 3. Device schematic of vertical β-Ga_2O_3 SBD on a conducting β-Ga_2O_3 substrate and (b) the SBD on β-$Ga_2O_3Ga_2O_3$ epi-layer on a conducting β-Ga_2O_3 substrate.

case. Various post-treatments are intended to reduce the interface states and to improve M−S contacts, attaining high performance with lower on-resistance (R_{ON}) and higher breakdown voltage (V_{BR}).

4. Ga_2O_3 power SBD

Early reports on Ga_2O_3 SBD devices have already shown very good rectification characteristics using a simple device structure without additional edge termination or other special structures [76]. Subsequently, along with different device structures and process regulation of Ga_2O_3 SBDs to carry out research work, a considerable number of properties have shown substantial improvement. It is noted that most of the reported parameters of device performance are with regard to breakdown voltage (V_{BR}), on-resistance (R_{ON}), forward current density (J_F) and reverse leakage (I_R). V_{BR} and R_{ON} are the two most important parameters, which indicate the maximum voltage that the device can withstand in reverse and the resistance value in forward conduction, respectively. By continuously optimizing materials and device structures, we are able to achieve Ga_2O_3 SBD products that meet commercial high-voltage (low-energy) requirements. Hence, this section summarizes the development of Ga_2O_3 power SBD in various metal choices, device structures, Ga_2O_3 material modification, and device processes.

4.1. The basic structure Ga_2O_3 SBD

For Ga_2O_3-based SBD devices, the initial devices were prepared with only front-side Schottky contacts and backside Ohmic contacts on a single crystal to study the device performance [37, 73, 75, 77]. The schematic of the device is shown in figure 3(a). An initial report by Sasaki *et al* [40] proposed the use of a Pt circular electrode Schottky junction to fabricate Pt/Ga_2O_3 SBD on single-crystal β-Ga_2O_3 (010) substrates. This device, using simple device structures and processing techniques without terminal structures and other processes demonstrates ideal coefficients close to 1.0. The SBH between Pt and β-Ga_2O_3 was 1.3–1.5 eV with a high breakdown voltage of about 150 V. These results can be attributed to the high crystal quality of Ga_2O_3 substrates and show the great potential of Ga_2O_3 power devices for future applications. These were further developed by adding an epitaxial layer to those early SBD structures. Pearton *et al* [78] reported that β-Ga_2O_3 SBDs were fabricated in a vertical structure on Si-doped epitaxial layers (10 μm, $n \approx 4 \times 10^{15}$ cm^{-3}) on Sn-doped bulk Ga_2O_3 substrates, which includes Ni/Au front Schottky contacts and Ti/Au back Ohmic contacts. The schematic of the device is shown in figure 3(b). It shows the device with V_{BR} values up to 1600 V (20 μm diameter contacts) and ~250 V for rectifiers (0.53 mm diameter), and R_{ON} values were 25 and 1.6 mΩ cm^2 respectively, leading to a BFOM for the latter of approximately 102.4 MW cm^{-2}. The results show that Ga_2O_3 SBDs without additional structures and edge terminals exhibit high performance based on high-quality substrates and epitaxy. The latest work presents a high-performance Ni/(001) β-Ga_2O_3 regular SBD without edge termination with a high PFOM of 1.32 GW cm^{-2} and a maximum V_{BR} of 1720 V by suppressing the formation of donor-like impurities accumulated on the surface [79]. Hence, Ga_2O_3 SBD has great potential for high-voltage applications.

Furthermore, the development of α-Ga_2O_3 SBD has achieved great success. In 2015, FLOSFIA, INC. [68] used mist CVD epitaxy to grow 8 μm thick n^+ epitaxial layer for Ohmic contact and n^- epitaxial layer for Schottky contact on sapphire substrate and then removed the sapphire substrate to make α-Ga_2O_3 SBD, as shown in figure 4(a). The device showed a V_{BR} of 270 V, n of 1.1 and a current on-off ratio of 10^6. The poor performance is caused by the current density limitation of the epitaxial layer. Afterwards, the conductivity of the α-Ga_2O_3 epitaxial layer was adjusted by controlling the doping of Sn to improve the performance of the SBD [80]. Two types of SBD were prepared, SBD 1 and SBD 2, of which SBD 1 with an n-epitaxial layer thickness of 430 nm exhibited low on-resistance (0.1 mΩ cm^2) and V_{BR} of 531 V; SBD 2

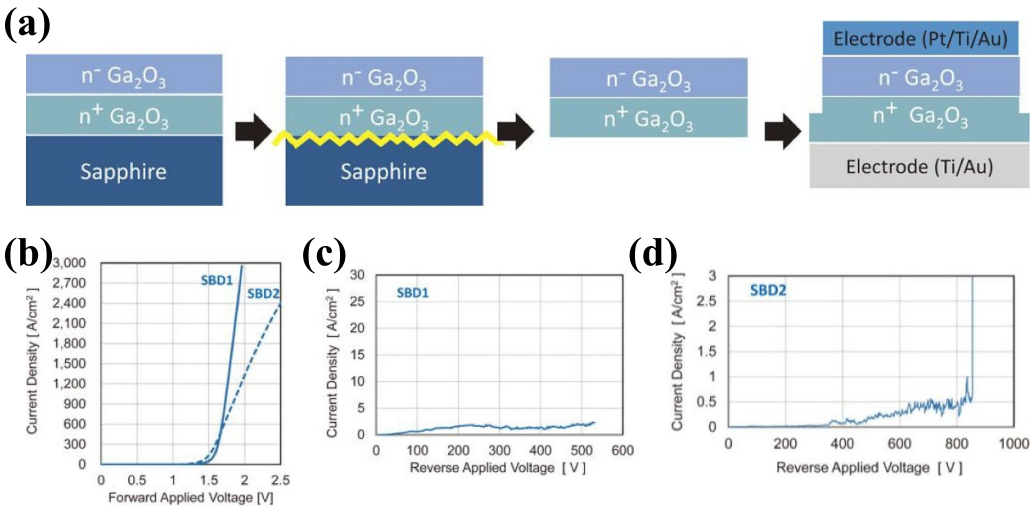

Figure 4. (a) Fabrication process of an α-Ga_2O_3 SBD. (b) Forward current density versus applied voltage characteristics of α-Ga_2O_3 SBDs. (c) Reverse current density versus applied voltage characteristics of α-Ga_2O_3 SBD1. (d) Reverse current density versus applied voltage characteristics of α-Ga_2O_3 SBD2. Reproduced from [80].

Table 3. Comparison of electrical performances for basic-structure Ga_2O_3 SBDs.

Device structure	Carrier concentration (cm^{-3})	V_{BR} (V)	V_{ON} (V)	R_{ON} (mΩ cm^2)	FOM (MW cm^{-2})	References
Pt/Ti/Au with UID substrate	3×10^{16} (600 μm)	150 (Φ100 μm)	1.23	7.85	3.1	[40]
Pt/Ti/Au with UID substrate	2.3×10^{14} ($\sim$600 μm)	>40 (Φ100 μm)	1.07	80	—	[73]
Au/Ti/Pt with substrate	2×10^{17} (0.48 μm)	200 (Φ150 μm)	0.63	2.9	—	[37]
Mo/Au with substrate	2×10^{17} (15 μm)	260 (Φ100 μm)	—	—	3	[75]
Ni/Au SBD	2×10^{16} (15 μm)	100 (0.1×0.3 cm^2)	—	23	0.435	[81]
	3.6×10^{18} (650 μm)	466 (40×40 μm^2)		0.59	368	
Pt/Ti/Au SBD	2×10^{16} (7 μm)	500 (Φ30 μm)	1.1	1	—	[72]
	2.5×10^{18} (—)					
Ni/Au SBD	2×10^{16} (10 μm)	1016 (Φ105 μm)		6	1.54×10^{-4}	[82]
	3.6×10^{18} (650 μm)					
Ni/Au SBD	4×10^{15} (10 μm)	1600 (Φ20 μm)	—	1.6–25	102.4	[78]
	3.6×10^{18} (650 μm)					
Ni/Au SBD	$\sim 1.2 \times 10^{16}$ (9 μm)	1720 (Φ100 μm)	—	2.25	1320	[79]
	3.6×10^{18} (—)					
Pt/Ti/Au SBD (α-Ga_2O_3)	1×10^{17} (0.43 μm)	532 (Φ30 μm)	—	0.1	—	[80]
	3×10^{19} ($3\sim4$ μm)					
	1×10^{17} (2.58 μm)	855 (Φ30 μm)	—	0.4	—	
	3×10^{19} ($3\sim4$ μm)					

with an n^- epitaxial layer thickness of 2580 nm exhibited a high breakdown voltage (855 V) and R_{ON} of 0.4 mΩ cm^2, as shown in figures 4(c) and (d). Both SBDs have an n^+ layer of 3–4 μm without edge termination, passivation or FP structure. The thermal resistance of the TO220-packaged α-Ga_2O_3 SBD device was found to be as small as 13.9 °C W^{-1}. This value is comparable to that of a commercial SiC SBD device (12.5 °C W^{-1}). This TO220-packaged α-Ga_2O_3 SBD also showed the fastest recovery compared to a commercial SiC SBD and a Si p−n junction diode [21]. This safe, low-cost and energy-efficient mist CVD epitaxial technology offers tremendous advantages for α-Ga_2O_3 power device applications. The comparison of electric performances for basic structure Ga_2O_3 SBDs are summarized in table 3.

4.2. Ga_2O_3 SBD with edge terminal processing

While there has been tremendous development of Ga_2O_3 devices, there are still many ways to improve device performance. Simple processes offer advantages in terms of industrialization and device reliability. Therefore, we want the fabrication process of Ga_2O_3-SBD to be as simple as possible. Ion-implantation terminal edge-termination technology can create a high-resistance region, thus forming effective electron isolation around the anode edge region. This effectively relieves the electric field crowding effect by reducing the peak value, as shown in figure 5(a). Therefore, the reported method of implementing ion-implanted edge termination, is a well-proven and effective way to increase the device

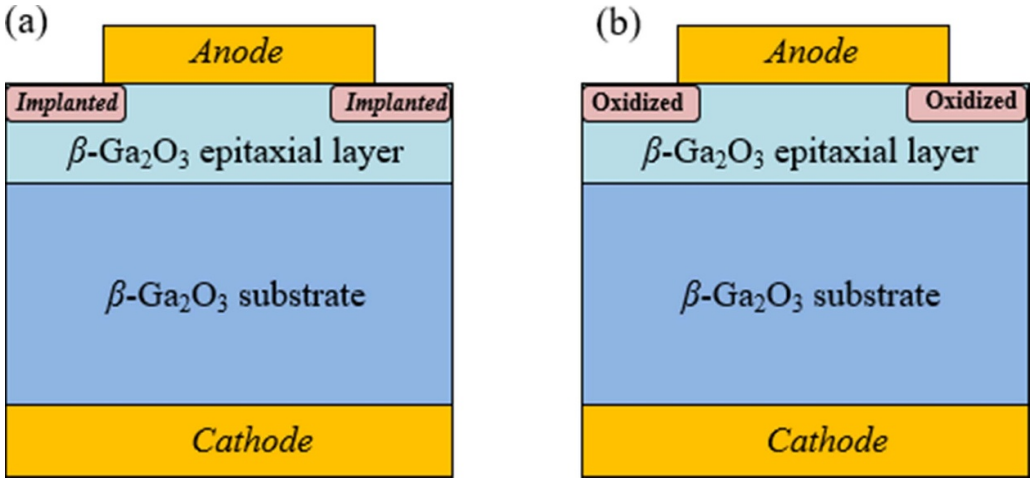

Figure 5. Device schematic of vertical β-Ga_2O_3 SBDs with (a) implanted edge termination, (b) thermally oxidized edge termination and (c) filled SiO_2 layer edge termination.

performance of Ga_2O_3-SBD. Zhou *et al* [83] reported that Mg-implanted edge-termination processing is a very simple but useful technique to improve the V_{BR} of the vertical β-Ga_2O_3 SBD. Compared to the device without Mg-implanted edge-termination treatment, the breakdown voltage of β-Ga_2O_3 SBD is substantially increased from 500 to 1050 V. In addition, it was shown that a high power figure of merit (PFOM) of 0.47 GW cm^{-2} and low R_{ON} of 5.1 mΩ cm^2 were realized at an epitaxial layer thickness of 10 μm with a diode radius of 90 μm. There is a slight increase in V_{BR} when the anode radius is decreased and a V_{BR} of 1.65 kV is demonstrated at $R = 40$ and 65 μm. To verify the effect of Mg-implanted edge termination on the device, technological computer-aided design (TCAD) simulations were carried out on the device with and without edge termination. The results showed the effectiveness of the implanted edge termination to mitigate the peak electric field at the anode edge and hence an enhanced breakdown voltage is expected. A similar approach is used to increase the breakdown voltage using an N-implanted guard ring [84]. The reverse leakage current is several orders of magnitude lower than the Mg-implanted edge-termination β-Ga_2O_3 SBD and the V_{BR} by up to 860 V. In addition, the Ga_2O_3 SBD was fabricated by using argon-implantation edge-terminated technology to form the high-voltage resistance performance at the periphery of the anode contacts [85, 86]. The results indicate great promise of vertical β-Ga_2O_3 SBDs for high-voltage and fast switching applications. The most recent reports on ion implantation to achieve high-performance vertical β-Ga_2O_3 SBD were based on a self-aligned beveled fluorine plasma treatment (BFPT) edge-termination structure [87]. Due to the strong electronegativity of fluorine ions, the introduction of numerous F negative charges will relieve the electric field pressure and therefore reduce reverse leakage and increase the breakdown voltage. The results indicate V_{BR} up to 1050 V with a relatively low R_{ON} of 2.5 mΩ cm^2, which is an excellent performance to date using a simple, effective and versatile edge-termination technique for self-aligned BFPT. This simple, easy-to-control edge-termination technique offers great advantages for fabricating high-quality, high-performance Ga_2O_3 SBD devices.

Wang *et al* [88] reported a novel edge-termination process to achieve a high-performance β-Ga_2O_3 vertical SBD by using thermally oxidized termination. The schematic of the device structure is shown in figure 5(b). The high-temperature thermal oxidation treatment reduces the electron concentration in the anode edge region and effectively suppresses the peak electric field at the device edge. For oxidation-terminated SBD annealed at 400 °C, the V_{BR} of β-Ga_2O_3 SBD increases from 380 to 940 V, but the R_{ON} only increases from 2.9 to 3.0 mΩ cm^2. The device demonstrates a PFOM (V_{BR}^2/R_{ON}) as high as 295 MW cm^{-2}. The decrease in the electron concentration in the oxidized region can effectively reduce the peak electric field at the Schottky contact edge. The simulation results of the lateral electrostatic field indicate that the thermally oxidized termination shows a new way to improve the breakdown characteristics of β-Ga_2O_3 SBD. Recently, Hao Yue's team reported a new terminal structure approach by incorporating the etched and filled SiO_2 layer process to obtain a record-high breakdown voltage of 6 kV and a low R_{ON} of 3.4 mΩ cm^2 for β-Ga_2O_3 SBD [89]. The device schematic is shown in figure 6. This simple and effective terminal structure allows Ga_2O_3 SBDs to be pushed to higher-voltage applications in power electronics.

In general, the edge-termination technique is the simplest, most effective and most versatile to achieve a termination cutoff at the edge of the device, which effectively increases V_{BR} and improves electrical properties at the electrode, by reducing the edge electron concentration and alleviating peak electric field. Therefore, this is greatly advantageous in preparing high-quality Ga_2O_3 SBD devices by using the simplest process possible. The comparison of electrical performances for β-Ga_2O_3 SBDs with edge termination (ET) are summarized in table 4.

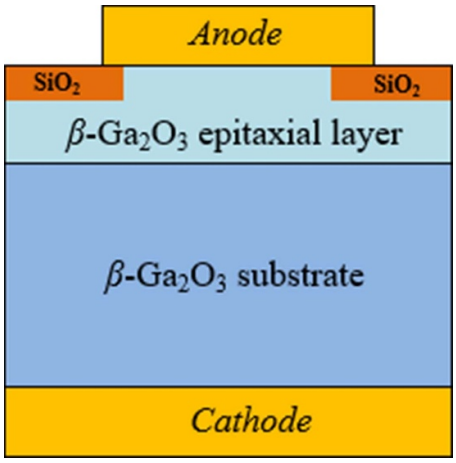

Figure 6. Device schematic of vertical β-Ga_2O_3 SBDs with filled SiO_2 layer edge termination.

Table 4. Comparison of electrical performances for β-Ga_2O_3 SBDs with edge termination (ET).

Device structure	Carrier concentration (cm^{-3})	V_{BR} (V)	V_{ON} (V)	R_{ON} (mΩ cm^2)	FOM (MW cm^{-2})	References
Ni/Au SBD with Mg-implanted ET	1.5×10^{16} (10 μm) 1.7×10^{19} (650 μm)	1550 (Φ90 μm)	0.82	5.1	470	[83]
Pt/Ni/Au SBD with N-implanted ET	$1\sim1.2 \times 10^{16}$ (7.8 μm) n+ (600 μm)	860 ($\sim\Phi$200 μm)	1.5	4.9	—	[84]
Ni/Au SBD with Ar-implanted ET	1.3×10^{17} (10 μm) n+ (600 μm)	451 (—)	1.5	3.3	61.6	[85]
Pt/Ti/Au SBD with Ar-implanted ET	4×10^{16} (8 μm) 2.6×10^{18} (640 μm)	391 (Φ100 μm)	1	4	—	[86]
Ni/Au/Ni SBD with beveled F-implanted ET	3×10^{16} (8 μm) 1.6×10^{19} (650 μm)	1050 (Φ100 μm)	0.7	2.5	—	[87]
Ni/Au SBD with thermally-oxidized termination	3×10^{16} (6 μm) 1.6×10^{19} (650 μm)	940 (Φ150 μm)	—	3	295	[88]
Ni/Au SBD with He-implanted ET	1.6×10^{16} (10 μm) 1.7×10^{19} (650 μm)	1000 (Φ65 μm)	0.73	4.8	210	[90]
Ni/Au SBD with Mg-implanted ET	1.6×10^{16} (10 μm) 1.7×10^{19} (650 μm)	1500 (Φ65 μm)	0.82	5.4	420	[90]
Ni/Au SBD with filled SiO_2 layer ET	1.3×10^{16} (10 μm) 3×10^{19} (500 μm)	6000 (Φ90 μm)	1.45	3.4	10 600	[89]
Pt/Au SBD with Compound ET	n− (7 μm) n+ (650 μm)	400 (Φ100 μm)	0.7	4	40	[91]

4.3. Ga_2O_3 SBD with field-plated structure

The effect of long-term Ga_2O_3 SBD device performance reliability due to damage to the lattice by ion implantation has not yet been studied. We need to find more ways to address the premature breakdown voltage of Ga_2O_3 SBDs due to the presence of a peak electric field at the electrode edges. Field-plated (FP) technology is widely used in AlGaN/GaN HEMTs, SiC, GaN and other power devices to improve the reverse breakdown voltage and electron distribution characteristics [92–97]. FP techniques have the advantage of a simpler and more controllable manufacturing process, and the fact that they avoid the increased leakage associated with ion implantation, ion implantation and thermal oxidation can create uncontrollable ion diffusion problems. The FP structure needs to be built on a dielectric layer, and the selection of a suitable dielectric layer will also determine device performance [62, 98]. The initial report on Ga_2O_3 field-plated SBDs (FP-SBDs) indicated that they were successfully fabricated on a Si-doped n^- Ga_2O_3 drift layer grown by HVPE on a Sn-doped n^+ Ga_2O_3 (001) substrate [99]. The $L_{FP} = 20$ μm FP Schottky anode electrodes were fabricated by realignment to the SiO_2 windows, as shown in figure 7(a). The results show that R_{ON} was estimated to be 5.1 mΩ cm^2 in a high V_{BR} of 1076 V, and the simulated maximum electric field below the anode foot edge was 5.1 MV cm^{-1}, as shown in figure 7(b). This is much larger than the theoretical limits for SiC and GaN and comparable to the extracted breakdown field for lateral Ga_2O_3 MOSFETs [100].

Yang *et al* are conducting a series of studies on Ga_2O_3 FP technology and comparing the differences in FP SBD with

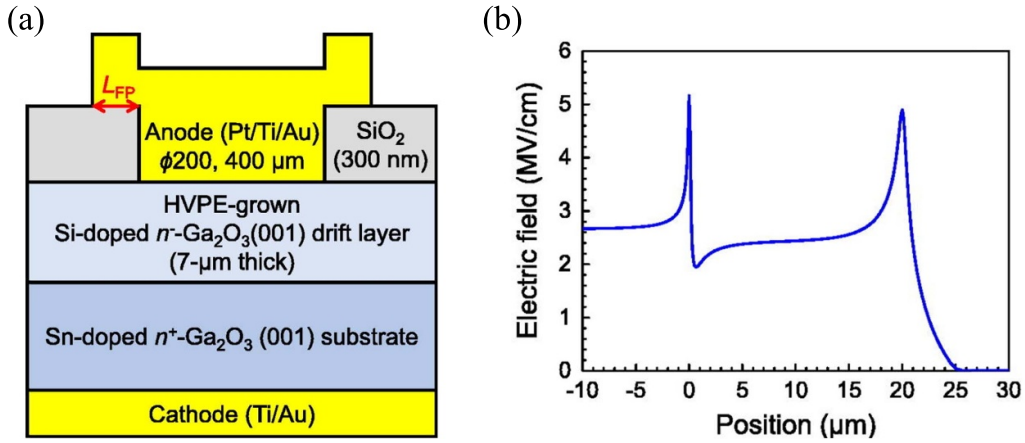

Figure 7. (a) Schematic cross-section of the Ga_2O_3 FP-SBD structure and (b) a maximum value of 5.1 MV cm^{-1} in the Ga_2O_3 drift layer at the anode foot edge. Reprinted from [99], with the permission of AIP Publishing.

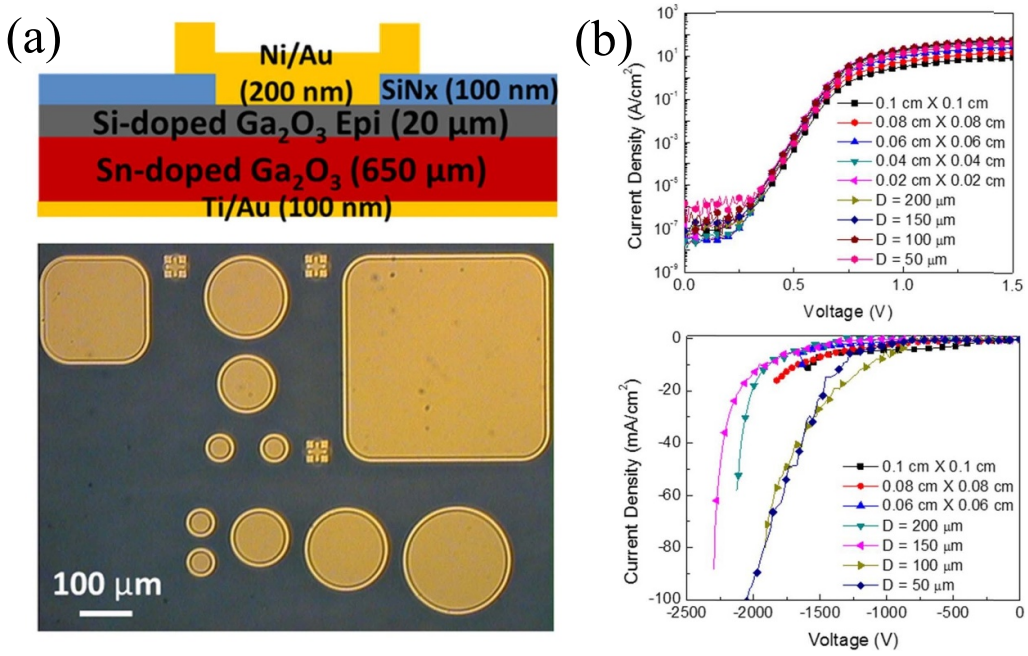

Figure 8. (a) Schematic of a vertical geometry Ni/Au Schottky rectifier with field-plate structure (top) and a top-view optical microscope image of the device layouts (bottom) showing different device areas. (b) Forward and reverse current density-voltage characteristic of rectifiers of different size (top). Reproduced from [103]. © 2018 The Electrochemical Society ("ECS"). Published on behalf of ECS by IOP Publishing Limited.

different dielectric layers [62, 101]. They initially prepared a Ga_2O_3 FP SBD with an electrode area of 0.01 cm^2 on a 10 μm thick, lightly doped drift layer (1.33×10^{16} cm^{-3}) on heavily doped (3.6×10^{18} cm^{-3}) substrates [102]. The device can achieve a forward current of 1 A and a reverse breakdown voltage of 650 V with a power density FOM above 20 MV cm^{-2}, which is well within the parameters of a power rectifier. Later, a new Ga_2O_3 FP SBD was prepared in A 20 μm thick, lightly doped ($n = 2.1 \times 10^{15}$ cm^{-3}) epitaxial layer on a conduction ($n = 3.6 \times 10^{18}$ cm^{-3}) substrate with a 150 μm diameter device (area $= 1.77 \times 10^{-4}$ cm^{-2}) [103]. The corresponding devices have further improved performance with breakdown voltages of up to 2300 V, as shown in figure 8. The on-state resistance (R_{ON}) for these devices was 0.25 Ω cm^2, leading to an FOM ($V_{BR}{}^2/R_{ON}$) of 21.2 MW cm^{-2} and can be adjusted to a voltage range of 1400–2300 V by changing the electrode size. In addition, a recovery time test with the device in the circuit showed a recovery time of only 20 ns from +2 to −2 V. In the future, the main focus will be on reducing the R_{ON} while continuing to increase the withstand voltage. To verify the application of the device in the circuit, the team prepared a switching circuit for high breakdown voltage Ga_2O_3 vertical Schottky rectifiers [104]. Based on this Ga_2O_3 FP SBD design, it can operate at switchable voltages of up to 900 V. Furthermore, a high-performance output current of 33.2 A and a PFOM ($V_{BR}{}^2/R_{ON}$) of 4.8 MW cm^{-1} were achieved through the array structure consisting of 21 Ga_2O_3 FP rectifiers [60]. These results are another milestone

Table 5. Comparison of electrical performances for β-Ga_2O_3 SBDs with field-plated (FP) structure.

Device structure	Carrier concentration (cm^{-3})	V_{BR} (V)	V_{ON} (V)	R_{ON} ($m\Omega\ cm^2$)	FOM ($MW\ cm^{-2}$)	References
Pt/Au/Ni SBD with beveled FP	2.5×10^{17} (2 μm) 3.6×10^{18} (650 μm)	190 (—)	—	0.023	—	[20]
Ni/Au SBD with FP	4.36×10^{15} (8 μm) 3.6×10^{18} (650 μm)	650 ($0.1 \times 0.1\ cm^2$)	—	0.518	26.5	[102]
Ni/Au SBD with FP	1.33×10^{16} (10 μm) 3.6×10^{18} (650 μm)	760 ($1.2 \times 1.2\ mm^2$)	—	22	26	[101]
Ni/Au SBD with FP	1.62×10^{16} (20 μm) 3.6×10^{18} (650 μm)	240 ($1 \times 1\ mm^2$)	2.9	12	4.8	[60]
Ni/Au SBD with FP	2.1×10^{15} (20 μm) 3.6×10^{18} (650 μm)	2300 (Φ150 μm)	—	0.25	21.2	[103]
Ni/Au SBD with small-angle beveled FP	3–3.5×10^{15} (10 μm) 2×10^{18} (400 μm)	1100 (Φ200 μm)	—	2	600	[105]
Ni/Au SBD with FP (600 K)	1.6×10^{16} (30 μm) n+ (650 μm)	750 ($40 \times 40\ \mu m^2$)		41	13.9	[106]
Ni/Au lateral film SBD with FP	2.9×10^{17} (600 nm)	2250 ($L_{AC} = 16\ \mu$m)		10.2	500	[107]
Pt/Ti/Au SBD with FP	1.8×10^{16} (10 μm) n+ (650 μm)	1076 (Φ200 μm)	1.32	5.1	223	[99]
Pt/Ti/Au SBD with FP and guard ring	$1 \sim 1.2 \times 10^{16}$ (7.8 μm) n+ (600 μm)	1430 (Φ200 μm)	1.6	4.7	—	[84]
Ni/Au SBD with high-k oxide FP	9×10^{16} (1.7 μm) conducting (—)	687 (Φ50 μm)	—	0.32	1470	[98]
Ni/Au SBD with beveled high-k oxide FP	3×10^{16} (8 μm) 2×10^{18} (2 μm)	3108 (Φ20 μm)	—	3.29	2940	[108]

for Ga_2O_3 towards its path for promising high-power electronic device applications since rectifiers are needed in inverter modules for power conversion systems.

Previously, beveled field-plate (BFP) Ga_2O_3 SBDs were also reported by Joshi *et al* [20] and Allen *et al* [105]. The latter reported better performance with the FP SBD, which consists of spin-on-glass and plasma-enhanced chemical vapor deposited SiO_2, to fabricate a very small bevel angle ($\sim 1^\circ$) in the mesa and FPs. The BFP SBD greatly promotes the electric field distribution at device edges, which results in a V_{BR} of 1100 V, a peak electric field of 3.5 MV cm^{-1},and a BFOM of 0.6 GW cm^{-2}. Xia *et al* [106] also investigated the performance of FP Ga_2O_3 SBDs at different temperatures, with reverse V_{BR} of 750 V at up to 600 K, 950 V at 500 K, and 1460 V at 400 K. Promising results of good protection against pressure and high-temperature operation were achieved. However, the FP-SBD device with the highest reverse breakdown voltage reported so far is a lateral structured device [107]. A high-performance lateral FP β-Ga_2O_3 SBD on a sapphire substrate with reverse V_{BR} of more than 3 kV and a low DC R_{ON} of 24.3 $m\Omega\ cm^2$ at an anode-cathode spacing (L_{AC}) of 24 μm is achieved. Overall, the external FP structure further improves the device's reverse breakdown voltage and exhibits a higher PFOM than the edge-termination structure.

In brief, FP structure techniques have been widely used in the fabrication of Ga_2O_3 power devices due to their relatively simple preparation process as well as the introduced external defects that cause increased reverse leakage. In order to implement the advantages of this FPe technology, more suitable high-dielectric materials are needed. In this way, FPs effectively reduce the peak value of the electric field at the edges of the channel. This will achieve a high breakdown voltage in Ga_2O_3 power devices. The comparison of electric performances for β-Ga_2O_3 SBDs with field-plated (FP) structure are summarized in table 5.

4.4. Ga_2O_3 SBD with trench structure

For conventional SBDs, the maximum electric field is located at the Schottky contact with surface higher reverse leakage current density at reverse bias, which means that limiting the electric field near the Schottky contact surface is necessary [109]. At present, various techniques, such as edge termination and FP structure, have been utilized to increase the V_{BR} of Ga_2O_3 SBDs by slowing down the peak electric field at the edge of the electrode. However, a large reverse leakage current is present, under a large reverse electric field, at the Schottky metal–semiconductor interface with a single junction barrier [110]. To alleviate the leakage constraint and the distribution of the maximum field strength from the Schottky contact surface to the inside of the device body, many power devices use junction-barrier-Schottky (JBS) structures with p–n junctions to reduce the electric field near the Schottky contact interface due to the charge-coupling effect [111]. However, since the problem of Ga_2O_3 p-type technology has not been resolved, the Ga_2O_3 SBD will not be able to adopt the JBS structure either. Trench MOS structure of the SBD will be a good choice, and the MOS junction on the sidewall will replace the p–n junction in the JBS [112–114]. Here, the introduction of a metal-insulator-semiconductor (MOS/MIS) junction barrier

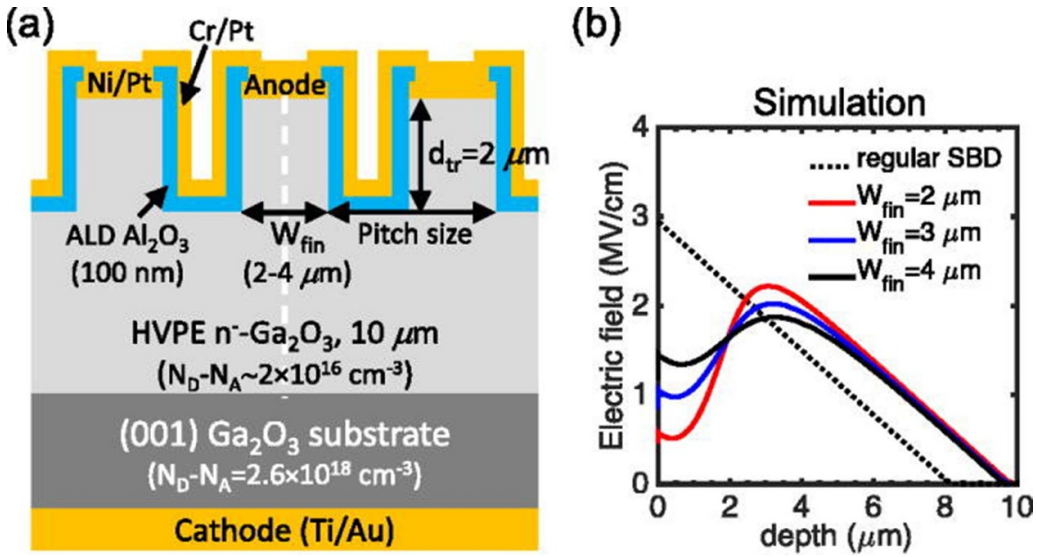

Figure 9. (a) Schematic cross-section of the β-Ga2O3 trench SBD with fin widths of 2, 3 and 4 μm, and trench depth of 2 μm. (b) Simulated electric field profile at a reverse bias of 1200 V along vertically cut lines at the center of the fins [see the dashed line in (a)]. Electric field profile in a regular SBD is shown by the dotted line for comparison. Reprinted from [118], with the permission of AIP Publishing.

structure not only increases the V_{BR} with trench termination, but also effectively reduces leakage with reduced surface electric field (RESURF) techniques.

Sasaki *et al* [115] first reported the Ga_2O_3-Trench-MOS SBD. The SBD was fabricated on a 7 μm (001) epitaxial layer ($n = 6 \times 10^{16}$ cm^{-3}) grown by halide vapor phase epitaxy (HVPE) on a single-crystal Ga_2O_3 substrate. Compared to the normal SBDs ($R_{ON} = 2.3$ mΩ cm^2), the R_{ON} (2.9 mΩ cm^2) is slightly higher, probably due to the reduced current path in the trench-MOS structure. The trench-MOS SBD has a leakage current several orders of magnitude smaller than the normal SBD, indicating that the trench MOS structure can effectively reduce the reverse leakage current. The device was tested for recovery characteristics by the double-pulse method [116]. It was confirmed that the trench MOS-Ga_2O_3-SBDs exhibit high speed and low loss recovery characteristics.

Many processing conditions affect the performance of the device, such as the appropriate thickness of the epitaxial layer, doping concentration, fin width, trench width, etc, which determine its final performance. In 2018, at the 76th Device Research Conference, it was reported that a trench-MIS device on 10 μm Si-doped n-Ga_2O_3 epitaxial layer grown on f 620 μm (001) n-type substrate, exhibited V_{BR} of 1.5 kV with a $\sim 10^4$ times reduction in reverse leakage current compared to regular SBDs [117]. Increasing the doping concentration of the epitaxial layer results in an increase in the forward current and a decrease in V_{BR} (1230 V) [118]. However, it maintains non-declining forward characteristics compared to regular SBD with trench structure, indicating that the trench structure has a significant effect in reducing the surface electric field and effective MOS junction barrier height. Figure 9(a) shows the schematic cross-section of the trench SBDs with fin widths of 2, 3 and 4 μm, and trench depth of 2 μm, where the trench region uses MIS (MOS)-junction structure. As shown in figure 9(b), the electric field near the top surface is effectively reduced by the trench-MIS structure, and the RESURF effect is more pronounced with a smaller fin width. The trench depth is further reduced to 1.5 μm, and after dry etching in BCl_3/Ar, the trench is then wet treated to remove the dry etch-induced damage and round the trench corners, resulting in devices with breakdown voltages of up to 2440 V and leakage current densities below 1 μA cm^{-2} [119].

To further improve the reverse breakdown voltage of Ga_2O_3 SBDs, Huang *et al* [120] used TCAD simulations for optimization to investigate the effect of structural parameters on V_{BR} and FOM based on the electric field distribution and edge effects at the bottom of the trench. As shown in figure 10, an optimized parameter of $W = 4$ μm and $R = 1.2$ μm, a maximum V_{BR} of over 3 kV and a FOM of 2 GW cm^{-2} are predicted. As the structural patterns of Ga_2O_3 SBDs develop, and the breakdown mechanism is better understood, experiments are considered to adopt some composite structures to further improve the performance of the devices. An FP-trench SBD was fabricated with a double dielectric layer, and the trench structure was adapted with a fin width of 1 μm and a fin height of 1.1 μm [121]. From a simulation analysis of the FP-trench structure with a surface, it is shown that the FP largely eliminates the peak electric field at the anode edge and moves the peak electric field location to the outer edge of the FP. Compared to previous reports ($V_{BR} = 2400$ V), this further increases the V_{BR} of the SBD to 2.48 kV and achieves a FOM value of 0.78 GW cm^{-2} by pulse testing. By further optimizing the previous device, both the fin and the trench width are designed to be 1 μm, together with the edge FP structure [122]. The device exhibits a high V_{BR} of 2.89 kV with a record high BFOM value of 0.80 (0.95) GW cm^{-2}, among all Ga_2O_3 power devices reported so far. In general, the trench-MOS barrier structure effectively reduces the electric field in the plane, resulting in a much lower reverse leakage and a higher breakdown voltage, which compensates for the material limitations that make it difficult to implement the p-type. Next, with a suitable edge-termination structure,

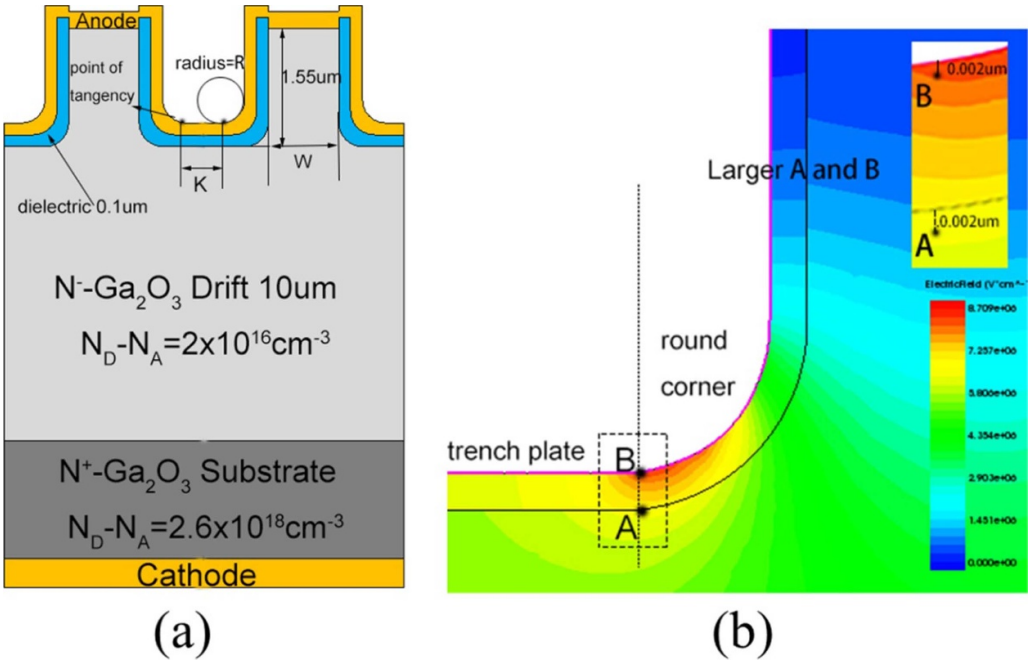

Figure 10. (a) Schematic of the SBD structure. (b) Electric field distribution and field strength gradient with a reverse bias for the Ga_2O_3 drift region E(A) and dielectric layer E(B). Reproduced from [120]. © IOP Publishing Ltd. CC BY 3.0.

Table 6. Comparison of electrical performances for β-Ga_2O_3 SBDs with trench structure.

Device structure	Carrier concentration (cm^{-3})	V_{BR} (V)	V_{ON} (V)	R_{ON} ($m\Omega\ cm^2$)	FOM ($MW\ cm^{-2}$)	References
Cu/Au/Ni SBD with MOS trench	6×10^{16} (7 μm) 2.5×10^{18} (350 μm)	240 (Φ400 μm)	—	2.9	—	[115]
Mo/Ni/Al SBD with MOS trench	6×10^{16} (7 μm) 5×10^{18} (500 μm)	300 (Φ300 μm)	0.5	3.09	—	[116]
Ni/Pt SBD with MIS trench	$\sim 2 \times 10^{16}$ (10 μm) 2.6×10^{18} (—)	1232 ($W_{fin} = 2$ μm)	—	15	—	[118]
Ni/Ti/Pt SBD with MIS trench	2×10^{16} (10 μm) 5.9×10^{18} (—)	2440 ($W_{fin} = 1$ μm)	1.25	11.3	390	[119]
SBD with optimized trench corner radius	2×10^{16} (10 μm) 2.6×10^{18} (—)	3400 ($W_{fin} = 1$ μm)	—	6	1700	[120]
Ni/Ti/Pt SBD with FP MOS trench	$\sim 1.47 \times 10^{16}$ (8.9 μm) 6.8×10^{18} (—)	2330 ($W_{fin} = 1$ μm)	—	7	780	[121]
Ni/Ti/Pt SBD with FP MOS trench	$\sim 1.47 \times 10^{16}$ (8.9 μm) 6.8×10^{18} (—)	2890 ($W_{fin} = 1$ μm)	—	8.8	950	[122]
Pt/Ti/Au SBD with trench staircase FP	2×10^{16} (8.5 μm) 6.8×10^{18} (—)	1660 ($W_{fin} = \Phi 200$ μm)	2.1	7.6	—	[123]
Ni/Ti/Pt SBD with FP MOS Trench	$\sim 7 \times 10^{15}$ (8.45 μm) 5.9×10^{18} (—)	2400 ($W_{fin} = 1$ μm)	1.25	20	—	[124]

it is believed that the performance of the device can be further improved.

Obviously, the trench-MOS structure of Ga_2O_3 is the preferred mode in kilovolt-level SBD devices with the base material p-type unresolved. The RESURF effect in trench-MOS structure not only improves the reverse leakage very well, but also improves the breakdown voltage to a great extent. However, there are still some details that need to be further investigated to reach an optimal device performance, such as optimization of the trench structure, suitable high-k dielectric layers and other process treatments. Together with other end-processing and FP structures, Ga_2O_3 SBD will have a huge potential in power devices. The comparison of electric performances for β-Ga_2O_3 SBDs with trench are summarized in table 6.

4.5. Other Ga_2O_3-based diodes (p–n HJDs)

Although the unipolar Ga_2O_3 SBD device has been significantly developed, the difficulty of p-type doping has limited the development of Ga_2O_3 p–n power diodes. Early reports use other p-type materials to construct Ga_2O_3 p–n HJDs to

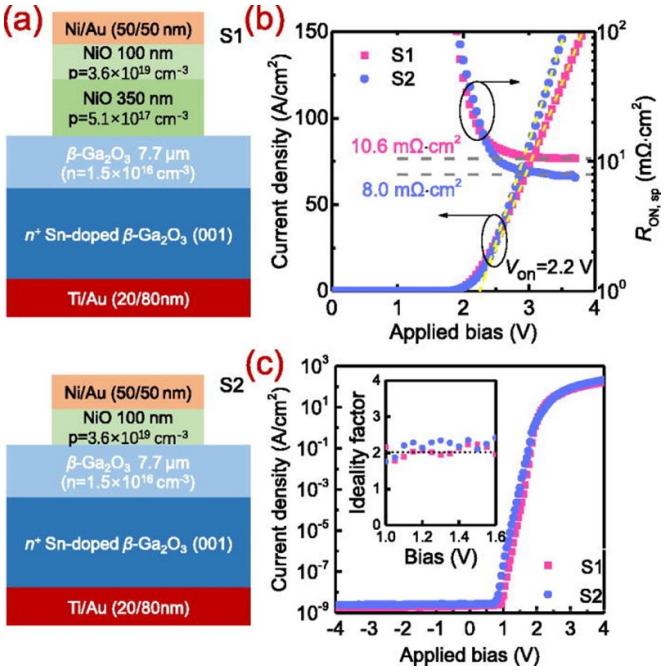

Figure 11. (a) Cross-section schematic of vertical NiO/β-Ga_2O_3 heterojunction diodes with two structural designs: (b) linear plots of J–V characteristics and extracted R_{ON} versus forward bias, where the turn-on voltage is obtained by fitting the linear segment and (c) semi-logarithmic plots of the J–V characteristics. Inset of (c) illustrates the extracted ideality factor. Reprinted from [129], with the permission of AIP Publishing.

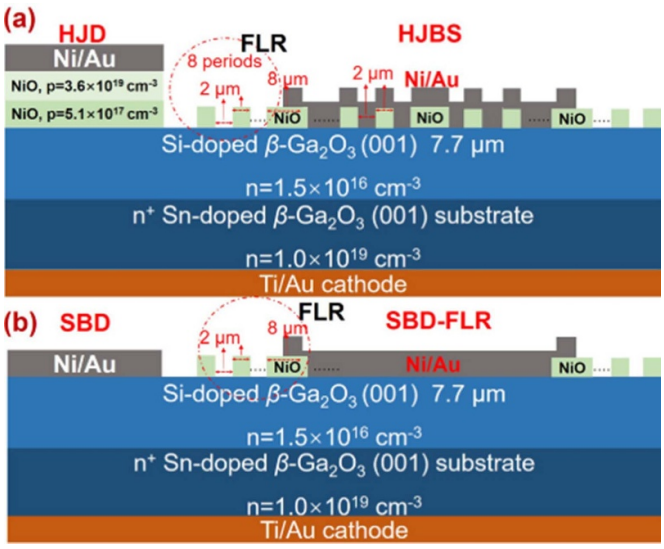

Figure 12. Schematics of vertical NiO/Ga_2O_3 p–n HJD, Ni/Ga_2O_3 SBD and HJBS-2 μm diode terminated with p-NiO FLRs and Ni/Ga_2O_3 SBD terminated with p-NiO FLRs. Width of the first p-NiO FLR is 8 μm, those of the other p-NiO rings are 2 μm, and all the p-NiO ring spacings are 2 μm. Reprinted from [133], with the permission of AIP Publishing.

achieve Ga_2O_3 bipolar power devices [125–127]. At this point, the heterojunction p-Cu_2O/Ga_2O_3 diode already exhibits a very high breakdown voltage of 1.49 kV and has a very high forward current of over 100 A cm^{-2} [127]. Considering that the narrow band gap of p-Cu_2O limits its potential, the p-NiO/Ga_2O_3 diodes also exhibit a high breakdown field strength of 1059 V and have an ultra-low reverse leakage current of below 1 μA cm^{-2} [128]. Ye *et al* [129] constructed a double-layered NiO/Ga_2O_3 vertical p–n HJD with different hole concentrations, as shown in figure 11. The device exhibits a very low leakage current and has a high rectification ratio of over 10^{10} (at $\pm$3 V) even when operated at a temperature of 400 K, indicating its excellent thermal stability and operation capability at high temperatures. The breakdown voltage has also greatly improved to 1.86 kV with R_{ON} of 10.6 mΩ cm^2.

The devices have been tested on circuits up to 12 A/70 A and have achieved ultra-fast switching performance with a reverse recovery time of 11 ns at a surge-current of 45 A [130]. This gives the device significant potential for high-voltage, high-frequency applications. In addition, some studies have shown that the annealed NiO/Ga_2O_3 p–n junctions have a very low defect density and that the performance of the diode is significantly improved [131]. As the research progressed, the first vertical β-Ga_2O_3 JBS diode was prepared, using the thermally oxidized p-type NiO to compensate for the absence of the p-type β-Ga_2O_3 [132]. The JBS diode exhibits a high electrical performance with V_{BR} of 1715 V and R_{ON} of 3.45 mΩ cm^2, yielding a BFOM ($V_{BR}{}^2/R_{ON}$) of 0.85 GW cm^{-2}, which is the highest direct-current FOM value among all β-Ga_2O_3 diodes. Meanwhile, a large-size JBS diode with an area of 1 $\times$ 1 mm^2 shows forward current I_F and V_{BR} of 5 A/700 V, which is also the best power factor (FOM = 64 MW cm^{-2}) among all published results about large-area Ga_2O_3 diodes. Next, in order to carry out a comparative study, five types of P-NiO/Ga_2O_3 heterojunction power SBDs with different configurations were fabricated, which include the heterojunction p-NiO/Ga_2O_3 JBS uniform field-limited ring width/spacing of 2 μm (HJBS-2 μm), HJBS-3 μm, Ni/Ga_2O_3 SBD with a uniform field limiting rings (SBD-FLR), NiO/Ga_2O_3 p–n HJD and Ni/Ga_2O_3 bare SBD, as shown in figure 12. HJBS-2 μm achieves a maximum V_{BR} of 1.89 kV and an R_{ON} of 7.7 mΩ cm^2, yielding a high FOM of 0.46 GW cm^{-2}. At the same time, the reverse leakage mechanism of HJBS is revealed to be Poole–Frenkel emission through localized trap states [133]. Recently, they have made a new breakthrough by reporting a novel composite terminal structure, including a p-type NiO junction termination extension and a small-angle BFP, which shows a much higher V_{BR} of 2410 V and a low R_{ON} of 1.12 mΩ cm^2, yielding a record-high power FOM value of 5.18 GW cm^{-2} [134]. In addition, p-GaN is also a good choice for constructing GaN/Ga_2O_3 p–n diodes with a low lattice mismatch of 2.6% [135], but there is little experimental research on GaN/Ga_2O_3 p–n power devices due to the fabrication limitations of GaN on Ga_2O_3. However, Nandi *et al* used TCAD simulations to propose a calibration model for the p-GaN/n-Ga_2O_3 junction barrier Schottky diode (JBSD) in Silvaco ATLAS. The JBSD provides better performance in terms of breakdown with a highest reverse breakdown voltage of 1890 V and a best switching time of 9.2 ns [136]. In fact, the heterojunction p–n also shows good performance and will be further developed when the p-type Ga_2O_3 problem is

Table 7. Comparison of electrical performances for β-Ga_2O_3 SBDs with p–n heterojunction structure.

Device structure	Carrier concentration (cm^{-3})	V_{BR} (V)	V_{ON} (V)	R_{ON} (mΩ cm^2)	FOM (MW cm^{-2})	References
p-Cu_2O/n-Ga_2O_3 diodes	$>10^{18}$ (200 nm) 4×10^{18} (10 μm)	1490 (Φ100 μm)	1.7	8.2	—	[127]
p-NiO/n-Ga_2O_3 diodes	1×10^{19} (200 nm) 4×10^{16} (8 μm) 2.6×10^{18} (—)	1059 (Φ200 μm)	1.2	3.5	—	[128]
Double-layered p-NiO/n-Ga_2O_3 diodes	3.6×10^{19} (100 nm) 5.1×10^{17} (300 nm) 1.5×10^{16} (7.7 μm) n+(—)	1860 (Φ200 μm)	2.2	10.6	330	[129]
Double-layered p-NiO/n-Ga_2O_3 diodes	1.7×10^{19} (100 nm) 5.1×10^{17} (300 nm) 2×10^{16} (10 μm) n+(—)	1370 (1 mm^2)	1.73	2.6	720	[130]
p-NiO/n-Ga_2O_3 diodes	1×10^{19} (300 nm) 2×10^{16} (10 μm) 5×10^{18} (640 μm)	1630 (Φ100 μm)	1.65	4.1	650	[131]
p-NiO/n-Ga_2O_3 JBS diodes	1×10^{18} (60 nm) 2×10^{16} (9 μm) 5×10^{18} (—)	1715 (100×100 μm^2)	1	3.45	850	[132]
p-NiO/n-Ga_2O_3 JBS diodes with field-limiting rings	1×10^{18} (280 nm) 1.5×10^{16} (7.7 μm) 1×10^{19} (—)	1890 (Φ200 μm)	1.1	7.7	460	[133]
p-NiO/n-Ga_2O_3 diodes with composite termination	1×10^{18} (80 nm) 1.8×10^{16} (6 μm) 1×10^{19} (650 μm)	2410 (Φ60 μm)	1.6	1.12	5180	[134]

not resolved. The comparison of electric performances for β-Ga_2O_3 SBDs with p-n heterojunction structure are summarized in table 7.

4.6. Brief summary on SBDs

In this section, we introduce several different structures of Ga_2O_3 SBDs and detail a few of the current best-performing devices. At present, some of the most basic devices have breakdown voltages close to 1000 V and may play an important role in the low and medium power market. However, to further increase the device's withstand voltage, other structures must be used, such as FPs, trench-MOS, etc. In addition, high-quality materials are an important part of improving device performance. Therefore, the combination and optimization of all mentioned factors can lead to further improvement of the performance of Ga_2O_3 SBD. With the development of Ga_2O_3 devices, the following improved points should be focused on.

4.6.1. High-quality material base. High-quality single crystal substrates and epitaxial films with controlled carrier concentration are the basic guarantee of outstanding and stable performance of Ga_2O_3 SBD. In particular, the high crystallinity and film uniformity exhibit a more consistent breakdown field strength, which prevents premature breakdown of the device. In addition, surface roughness and crystal defects are used as key factors to improve the properties of electrical conductivity and leakage of the device. Furthermore, a largesize wafer (>4 inches) is a basic requirement for industrialization, which can accelerate the industrialization of Ga_2O_3 devices. The solution of the p-type Ga_2O_3problem will open another window to Ga_2O_3-based power devices, which will enable further improvement. Therefore, the development of Ga_2O_3 materials is crucial as the cornerstone of device development.

4.6.2. Contact interface of metal/Ga_2O_3. The contact between metal and Ga_2O_3 is the main determinant of electron transport between interfaces and further affects the performance of the device. A proper Schottky and Ohmic contact will be a key factor in influencing the forward and reverse electron transfer characteristics of the device. In addition, the I–V electronic characteristic curve can also be further improved by the contact interface, for example, high-k materials in trench-MOS structures can improve reverse leakage. Other suitable interfacial treatments will also be beneficial to improve the electron transfer characteristics, such as plasma treatment and interface annealing.

4.6.3. Device structure optimization. The process of adding additional structure allows the Ga_2O_3 SBD to develop towards higher breakdown voltages, but the details of the structure still need to be further studied to achieve optimal performance. As mentioned above, the edge-termination structure

and FP structure can effectively reduce the peak electric field at the verge of catastrophic breakdown, and effectively improve the breakdown characteristics. The trench-MOS barrier structure also has great advantages in reducing reverse leakage and increasing breakdown voltage. Consequently, a continuous structural optimization and combination will provide enhanced performance.

4.6.4. Device thermal management. Due to the low thermal conductivity of Ga_2O_3 itself, Ga_2O_3 SBD suffers from a severe self-heating effect. The performance degradation will be greatly impacted under long-term high-temperature operation of Ga_2O_3-based devices. In particular, high-temperature operation can lead to severe current leakage and result in a decline in device reliability. A promising solution is to construct β-Ga_2O_3 heterojunctions integrated onto a high thermal conductivity substrate [137–140]. Xu *et al* reported the wafer-scale exfoliation of β-Ga_2O_3 thin films by an ion-cutting technique with H implantation and transfer onto 4H-SiC and Si substrates with high thermal conductivity. This avoids causing poor quality of the hetero-epitaxy-grown film due to the large lattice mismatch [141–145]. Compared to bulk Ga_2O_3 wafer, it demonstrated a fine performance improvement in leakage current and breakdown voltage and better thermal stability. However, most SBDs are vertical structures and it is clear that this method of transferring to a high-dielectric layer, high-conductivity substrate is not applicable. The fact is that there are already many ways to solve this problem with thermal management. For example, the double-sided packaging of Ga_2O_3 Schottky rectifiers exhibits a low thermal resistance of 0.5 K W^{-1} [146, 147]. We believe there will be more ways to solve the heat dissipation problem of Ga_2O_3 in the future.

4.6.5. Device reliability. In order to achieve reliable applications of power Ga_2O_3 SBDs, it is important to investigate the reliability of the device over time and temperature. Some researchers report that temperature plays an important factor. A long-term high-temperature operation will lead to an increase in the current density and cause electrode metal degradation, and also induce an increase in the concentration of defects, which can seriously affect the normal operation of the device and even lead to device failure [148, 149]. The long-term reliability of Ga_2O_3 power diode operational capabilities in electronic power circuits will be an unavoidable challenge. Zhou *et al* [150] performed reliability verification of beveled-mesa NiO/β-Ga_2O_3 HJD after over one million times dynamic breakdown with a 1.2 kV peak overvoltage. The results showed that the reverse blocking characteristics caused no significant degradation and the beveled-mesa NiO/Ga_2O_3 p–n HJDs achieved a high conversion efficiency of 98.5% with 100 min stable operating capability into a 500 W power factor correction system circuit. Of course, there are few reports of reliability verifications like this, and further exploration of the reliability of Ga_2O_3-based power devices is needed to promote industrial applications.

5. Summary and prospects

In this review, we summarize recent advanced reports on Ga_2O_3-based SBDs. Due to the intrinsic superiority of the Ga_2O_3 material, it has great potential for the development of power devices and is expected to be one of the dominant materials used in the power electronics market, comparable to GaN and SiC. At present, Ga_2O_3 SBDs are in a rapidly developing stage, with breakdown voltage records that keep being broken. Thus, Ga_2O_3 SBDs have great prospects with the premise of ensuring the maturity of the material.

With the continuous development of semiconductor materials and the advent of the post-Moore era, wide-band semiconductors are destined to become the new choice in an era of rapid information technology development. Nevertheless, the properties of Ga_2O_3 and relevant microelectronics are still at early stages and need to be clarified. The development of Ga_2O_3 is still full of prospects and opportunities. Together with optimizing materials and structures to improve Ga_2O_3 SBD performance, the following points may be of interest.

(a) To date, most of the research on Ga_2O_3 power devices has been on β phase. Other phase power devices will also be an interesting research direction in the future.
(b) Compared to SiC, Ga_2O_3 SBD has already reached a relatively high level of withstand voltage. The next step is to continue to improve the withstand voltage and at the same time, we should increase the research on reducing the on-state resistance and verify the reliability of the device.
(c) We still require a better thermal management method of Ga_2O_3 to solve the problem of poor thermal conductivity.

Data availability statement

No new data were created or analyzed in this study.

Acknowledgments

This work was funded by the National Natural Science Foundation of China (Grnat Nos. 61774019 and 61704153), the State Key Laboratory of Information Photonics and Optical Communications (Grant No. IPOC2018ZZ01) (Beijing University of Posts and Telecommunications) and the Fundamental Research Funds for the Central Universities, China.

ORCID iDs

Xueqiang Ji https://orcid.org/0000-0002-5623-2957
Li Shan https://orcid.org/0000-0002-3095-3721
Zeng Liu https://orcid.org/0000-0003-3215-7929
Peigang Li https://orcid.org/0000-0002-3148-5050

References

[1] Hazra S, De A, Cheng L, Palmour J, Schupbach M, Hull B A, Allen S and Bhattacharya S 2016 High switching performance of 1700-V, 50-A SiC power MOSFET over

Si IGBT/BiMOSFET for advanced power conversion applications *IEEE Trans. Power Electron.* **31** 4742–54
[2] Chen K J, Haberlen O, Lidow A, Tsai C L, Ueda T, Uemoto Y and Wu Y 2017 GaN-on-Si power technology: devices and applications *IEEE Trans. Electron Devices* **64** 779–95
[3] Zhang L, Yuan X, Wu X, Shi C, Zhang J and Zhang Y 2019 Performance evaluation of high-power SiC MOSFET modules in comparison to Si IGBT modules *IEEE Trans. Power Electron.* **34** 1181–96
[4] Rujas A, López V M, Garcia-Bediaga A, Berasategi A and Nieva T 2019 Railway traction DC–DC converter: comparison of Si, SiC-hybrid, and full SiC versions with 1700 V power modules *IET Power Electron.* **12** 3265–71
[5] Chow T P 2006 High-voltage SiC and GaN power devices *Microelectron. Eng.* **83** 112–22
[6] She X, Huang A Q, Lucia O and Ozpineci B 2017 Review of silicon carbide power devices and their applications *IEEE Trans. Ind. Electron.* **64** 8193–205
[7] Treu M, Rupp R, Blaschitz P and Hilsenbeck J 2006 Commercial SiC device processing: status and requirements with respect to SiC based power devices *Superlattices Microstruct.* **40** 380–7
[8] Millan J, Godignon P, Perpina X, Perez-Tomas A and Rebollo J 2014 A survey of wide bandgap power semiconductor devices *IEEE Trans. Power Electron.* **29** 2155–63
[9] Jones E A, Wang F F and Costinett D 2016 Review of commercial GaN power devices and GaN-based converter design challenges *IEEE J. Emerg. Sel. Top. Power Electron.* **4** 707–19
[10] Pushpakaran B N, Subburaj A S and Bayne S B 2020 Commercial GaN-based power electronic systems: a review *J. Electron. Mater.* **49** 6247–62
[11] Yan H, Huang Y, Cui W, Zhi Y, Guo D, Wu Z, Chen Z and Tang W 2018 Magnetic properties and crystal structure of $Ga_{2-x}Fe_xO_3$ *Powder Diffr.* **33** 195–201
[12] Yoshioka S, Hayashi H, Kuwabara A, Oba F, Matsunaga K and Tanaka I 2007 Structures and energetics of Ga_2O_3 polymorphs *J. Phys.: Condens. Matter* **19** 346211
[13] Kuramata A, Koshi K, Watanabe S, Yamaoka Y, Masui T and Yamakoshi S 2016 High-quality β-Ga_2O_3 single crystals grown by edge-defined film-fed growth *Jpn. J. Appl. Phys.* **55** 1202A2
[14] Liu Z, Li P G, Zhi Y S, Wang X L, Chu X L and Tang W H 2019 Review of gallium oxide based field-effect transistors and Schottky barrier diodes *Chin. Phys.* B **28** 017105
[15] Pearton S J, Yang J, Cary P H, Ren F, Kim J, Tadjer M J and Mastro M A 2018 A review of Ga_2O_3 materials, processing, and devices *Appl. Phys. Rev.* **5** 011301
[16] Mastro M A, Kuramata A, Calkins J, Kim J, Ren F and Pearton S J 2017 Perspective—opportunities and future directions for Ga_2O_3 *ECS J. Solid State Sci. Technol.* **6** P356–9
[17] Stepanov S I, Nikolaev V I, Bougrov V E and Romanov A E 2016 Gallium oxide: properties and applications—a review *Rev. Adv. Mater. Sci.* **44** 63–86
[18] Alema F, Zhang Y, Osinsky A, Valente N, Mauze A, Itoh T and Speck J S 2019 Low temperature electron mobility exceeding 10^4 cm^2/V s in MOCVD grown β-Ga_2O_3 *APL Mater.* **7** 121110
[19] Zhang Y, Alema F, Mauze A, Koksaldi O S, Miller R, Osinsky A and Speck J S 2019 MOCVD grown epitaxial β-Ga_2O_3 thin film with an electron mobility of 176 cm^2/V s at room temperature *APL Mater.* **7** 022506
[20] Joishi C, Rafique S, Xia Z, Han L, Krishnamoorthy S, Zhang Y, Lodha S, Zhao H and Rajan S 2018 Low-pressure CVD-grown β-Ga_2O_3 bevel-field-plated Schottky barrier diodes *Appl. Phys. Express* **11** 031101
[21] Kaneko K, Fujita S and Hitora T 2018 A power device material of corundum-structured α-Ga_2O_3 fabricated by MIST EPITAXY® technique *Jpn. J. Appl. Phys.* **57** 02CB18
[22] Uchida T, Kaneko K and Fujita S 2018 Electrical characterization of Si-doped n-type α-Ga_2O_3 on sapphire substrates *MRS Adv.* **3** 171–7
[23] Chen Y, Xia X, Liang H, Abbas Q, Liu Y and Du G 2018 Growth pressure controlled nucleation epitaxy of pure phase ε- and and β-Ga_2O_3 films on Al_2O_3 via metal-organic chemical vapor deposition *Cryst. Growth Des.* **18** 1147–54
[24] Wei H, Chen Z, Wu Z, Cui W, Huang Y and Tang W 2017 Epitaxial growth and characterization of $CuGa_2O_4$ films by laser molecular beam epitaxy *AIP Adv.* **7** 3–10
[25] Kukushkin S A, Nikolaev V I, Osipov A V, Osipova E V, Pechnikov A I and Feoktistov N A 2016 Epitaxial gallium oxide on a SiC/Si substrate *Phys. Solid State* **58** 1876–81
[26] Sasaki K, Higashiwaki M, Kuramata A, Masui T and Yamakoshi S 2013 MBE grown Ga_2O_3 and its power device applications *J. Cryst. Growth* **378** 591–5
[27] Sasaki K, Higashiwaki M, Kuramata A, Masui T and Yamakoshi S 2013 Si-Ion implantation doping in β-Ga_2O_3 and its application to fabrication of low-resistance ohmic contacts *Appl. Phys. Express* **6** 086502
[28] Lee S D, Ito Y, Kaneko K and Fujita S 2015 Enhanced thermal stability of alpha gallium oxide films supported by aluminum doping *Jpn. J. Appl. Phys.* **54** 3–7
[29] Mi W, Ma J, Li Z, Luan C and Xiao H 2015 Characterization of Sn-doped β-Ga_2O_3 films deposited on MgO (100) substrate by MOCVD *J. Mater. Sci. Mater. Electron.* **26** 7889–94
[30] Chen Z, Saito K, Tanaka T and Guo Q 2017 Efficient pure green emission from Er-doped Ga_2O_3 films *CrystEngComm* **19** 4448–58
[31] Li W *et al* 2017 Structural, optical and photoluminescence properties of Pr-doped β-Ga_2O_3thin films *J. Alloys Compd.* **697** 388–91
[32] Masataka H, Kohei S, Hisashi M, Yoshinao K, Akinori K, Akito K, Takekazu M and Shigenobu Y 2016 Recent progress in Ga_2O_3 power devices *Semicond. Sci. Technol.* **31** 034001
[33] Dong H *et al* 2019 Fast switching β-Ga_2O_3 power MOSFET with a trench-gate structure *IEEE Electron Device Lett.* **40** 1385–8
[34] Hilt O, Treidel E B, Wolf M, Kuring C, Tetzner K, Yazdani H, Wentzel A and Würfl J 2019 Lateral and vertical power transistors in GaN and Ga_2O_3 *IET Power Electron.* **12** 3919–27
[35] Villora E G, Shimamura K, Yoshikawa Y, Aoki K and Ichinose N 2004 Large-size β-Ga_2O_3 single crystals and wafers *J. Cryst. Growth* **270** 420–6
[36] Tang X, Liu B, Yu Y, Liu S and Gao B 2021 Numerical analysis of difficulties of growing large-size bulk β-Ga_2O_3 single crystals with the Czochralski method *Crystals* **11** 763
[37] He Q *et al* 2018 Schottky barrier rectifier based on (100) β-Ga_2O_3 and its DC and AC characteristics *IEEE Electron Device Lett.* **39** 556–9
[38] Tung R T 2001 Recent advances in Schottky barrier concepts *Mater. Sci. Eng.* R **35** 1–138
[39] Li L, Liao F and Hu X 2020 The possibility of N–P codoping to realize P-type β-Ga_2O_3 *Superlattices Microstruct.* **141** 106502
[40] Sasaki K, Higashiwaki M, Kuramata A, Masui T and Yamakoshi S 2013 Ga_2O_3 schottky barrier diodes fabricated by using single-crystal β-Ga_2O_3 (010) substrates *IEEE Electron Device Lett.* **34** 493–5

[41] Li L, Wei W and Behrens M 2012 Synthesis and characterization of α-, β-, and γ-Ga_2O_3 prepared from aqueous solutions by controlled precipitation *Solid State Sci.* **14** 971–81

[42] Roy R, Hill V G and Osborn E F 1952 Polymorphism of Ga_2O_3 and the system Ga_2O_3-H_2O *J. Am. Chem. Soc.* **74** 719–22

[43] Mulazzi M, Reichmann F, Becker A, Klesse W M, Alippi P, Fiorentini V, Parisini A, Bosi M and Fornari R 2019 The pressure-induced phase transition of Ga_2O_3 *APL Mater.* **7** 10627–30

[44] Nikolaev V I, Stepanov S I, Pechnikov A I, Shapenkov S V, Scheglov M P, Chikiryaka A V and Vyvenko O F 2020 HVPE growth and characterization of ε-Ga_2O_3 films on various substrates *ECS J. Solid State Sci. Technol.* **9** 045014

[45] Kim S H, Yang M, Lee H Y, Choi J S, Lee H U, Kim U J and Lee M 2021 Structural characteristics of α-Ga_2O_3 films grown on sapphire by halide vapor phase epitaxy *Mater. Sci. Semicond. Process.* **123** 105534

[46] Pratiyush A S, Xia Z, Kumar S, Zhang Y, Joishi C, Muralidharan R, Rajan S and Nath D N 2018 MBE-grown β-Ga_2O_3-based Schottky UV-C photodetectors with rectification ratio $\sim 10^7$ *IEEE Photonics Technol. Lett.* **30** 2025–8

[47] Vogt P *et al* 2021 Adsorption-controlled growth of Ga_2O_3 by suboxide molecular-beam epitaxy *APL Mater.* **9** 031101

[48] Sun H, Li K H, Castanedo C G T, Okur S, Tompa G S, Salagaj T, Lopatin S, Genovese A and Li X 2018 HCl flow-induced phase change of α-, β-, and ε-Ga_2O_3 films grown by MOCVD *Cryst. Growth Des.* **18** 2370–6

[49] Li Z, Chen Z, Chen W and Wang G 2019 Phase control of Ga_2O_3 thin films grown by metal-organic chemical vapor deposition *Mater. Sci. Forum* **954** 72–76

[50] Xu C, Shen L, Liu H, Pan X and Ye Z 2021 High-quality β-Ga_2O_3 films with influence of growth temperature by pulsed laser deposition for solar-blind photodetectors *J. Electron. Mater.* **50** 2043–8

[51] Tan L, Zhang J, Guo X, Huang W, Deng C and Cui R 2021 Characterization of β-Ga_2O_3 films deposited under different growth temperature by pulsed laser deposition *J. Mater. Sci. Mater. Electron.* **32** 21044–51

[52] Tran H N, Le P Y, Murdoch B J, Allen M W, McConville C F and Partridge J G 2020 Temperature-dependent electrical properties of graphitic carbon Schottky contacts to β-Ga_2O_3 *IEEE Trans. Electron Devices* **67** 5669–75

[53] Mobtakeri S, Akaltun Y, Özer A, Kılıç M, Tüzemen E Ş and Gür E 2021 Gallium oxide films deposition by RF magnetron sputtering; a detailed analysis on the effects of deposition pressure and sputtering power and annealing *Ceram. Int.* **47** 1721–7

[54] Guo Y, Zhang J, Zhu F, Yang Z X, Xu J and Yu J 2008 Self-assembly of β-Ga_2O_3 nanobelts *Appl. Surf. Sci.* **254** 5124–8

[55] Cowley A M and Sze S M 1965 Surface states and barrier height of metal-semiconductor systems *J. Appl. Phys.* **36** 3212–20

[56] Wang Y *et al* 2021 Temperature-dependent characteristics of Schottky barrier diode on heterogeneous β-Ga_2O_3(−201)-Al_2O_3-Si substrate *J. Appl. Phys.* **54** 034004

[57] Lee M H and Peterson R L 2019 Interfacial reactions of titanium/gold ohmic contacts with Sn-doped β -Ga_2O_3 *APL Mater.* **7** 022524

[58] Tang W *et al* 2021 Temperature-dependent electrical characteristics of β-Ga_2O_3 trench Schottky barrier diodes via self-reactive etching *J. Appl. Phys.* **54** 425104

[59] Alema F, Hertog B, Mukhopadhyay P, Zhang Y, Mauze A, Osinsky A, Schoenfeld W V, Speck J S and Vogt T 2019 Solar blind Schottky photodiode based on an MOCVD-grown homoepitaxial β-Ga_2O_3 thin film *APL Mater.* **7** 022527

[60] Yang J *et al* 2019 Vertical geometry 33.2 A, 4.8 MW cm^2 Ga_2O_3 field-plated Schottky rectifier arrays *Appl. Phys. Lett.* **114** 232106

[61] Yao Y, Gangireddy R, Kim J, Das K K, Davis R F and Porter L M 2017 Electrical behavior of β-Ga_2O_3 Schottky diodes with different Schottky metals *J. Vac. Sci. Technol.* B **35** 03D113

[62] Carey P H, Yang J, Ren F, Sharma R, Law M and Pearton S J 2019 Comparison of dual-stack dielectric field plates on β-Ga_2O_3 Schottky rectifiers *ECS J. Solid State Sci. Technol.* **8** Q3221–5

[63] Bhattacharyya A, Roy S, Ranga P, Shoemaker D, Song Y, Lundh J S, Choi S and Krishnamoorthy S 2021 130 mA mm^{-1} β-Ga_2O_3 metal semiconductor field effect transistor with low-temperature metalorganic vapor phase epitaxy-regrown ohmic contacts *Appl. Phys. Express* **14** 076502

[64] Jeong Y J, Yang J Y, Lee C H, Park R, Lee G, Chung R B K and Yoo G 2021 Fluorine-based plasma treatment for hetero-epitaxial β-Ga_2O_3 MOSFETs *Appl. Surf. Sci.* **558** 149936

[65] Massabuau F, Nicol D, Adams F, Jarman J, Roberts J, Kovács A, Chalker P and Oliver R 2021 Study of Ti contacts to corundum α-Ga_2O_3 *J. Appl. Phys.* **54** 384001

[66] Suzuki R, Nakagomi S, Kokubun Y, Arai N and Ohira S 2009 Enhancement of responsivity in solar-blind β-Ga_2O_3 photodiodes with a Au Schottky contact fabricated on single crystal substrates by annealing *Appl. Phys. Lett.* **94** 3–6

[67] Mohamed M, Irmscher K, Janowitz C, Galazka Z, Manzke R and Fornari R 2012 Schottky barrier height of Au on the transparent semiconducting oxide β-Ga_2O_3 *Appl. Phys. Lett.* **101** 3–8

[68] Oda M, Kikawa J, Takatsuka A, Tokuda R, Sasaki T, Kaneko K, Fujita S, Hitora T, Plaza K V and Science E 2015 Vertical Schottky barrier diodes of a-Ga_2O_3 fabricated by mist epitaxy *2015 73rd Annual Device Research Conf.* pp 137–8

[69] Farzana E, Zhang Z, Paul P K, Arehart A R and Ringel S A 2017 Influence of metal choice on (010) β-Ga_2O_3 Schottky diode properties *Appl. Phys. Lett.* **110** 202102

[70] Irmscher K, Galazka Z, Pietsch M, Uecker R and Fornari R 2011 Electrical properties of β-Ga_2O_3 single crystals grown by the Czochralski method *J. Appl. Phys.* **110** 063720

[71] Splith D, Müller S, Schmidt F, Von Wenckstern H, Van Rensburg J J, Meyer W E and Grundmann M 2014 Determination of the mean and the homogeneous barrier height of Cu Schottky contacts on heteroepitaxial β-Ga_2O_3 thin films grown by pulsed laser deposition *Phys. Status Solidi* a **211** 40–47

[72] Higashiwaki M *et al* 2016 Temperature-dependent capacitance-voltage and current-voltage characteristics of Pt/Ga_2O_3 (001) Schottky barrier diodes fabricated on n^--Ga_2O_3 drift layers grown by halide vapor phase epitaxy *Appl. Phys. Lett.* **108** 133503

[73] He Q, Mu W, Dong H, Long S, Jia Z, Lv H, Liu Q, Tang M, Tao X and Liu M 2017 Schottky barrier diode based on β-Ga_2O_3 (100) single crystal substrate and its temperature-dependent electrical characteristics *Appl. Phys. Lett.* **110** 093503

[74] Fares C, Ren F and Pearton S J 2019 Temperature-dependent electrical characteristics of β-Ga_2O_3 Diodes with W Schottky contacts up to 500 °C *ECS J. Solid State Sci. Technol.* **8** Q3007–12

[75] Hu Z *et al* 2019 Experimental and theoretical studies of Mo/Au Schottky contact on mechanically exfoliated β-Ga_2O_3 thin film *Nanoscale Res. Lett.* **14** 2

[76] Sasaki K, Kuramata A, Masui T, Víllora E G, Shimamura K and Yamakoshi S 2012 Device-qualityβ-Ga_2O_3 epitaxial films fabricated by ozone molecular beam epitaxy *Appl. Phys. Express* **5** 14–17

[77] Fujita S, Oda M, Kaneko K and Hitora T 2016 Evolution of corundum-structured III-oxide semiconductors: growth, properties, and devices *Jpn. J. Appl. Phys.* **55** 1202A3

[78] Yang J, Ahn S, Ren F, Pearton S J, Jang S and Kuramata A 2017 High breakdown voltage (−201) β-Ga_2O_3 schottky rectifiers *IEEE Electron Device Lett.* **38** 906–9

[79] Qiming H *et al* 2022 Over 1 GW/cm^2 vertical Ga_2O_3 Schottky barrier diodes without edge termination *IEEE Electron Device Lett.* **43** 264–7

[80] Oda M, Tokuda R, Kambara H, Tanikawa T, Sasaki T and Hitora T 2016 Schottky barrier diodes of corundum-structured gallium oxide showing on-resistance of 0.1 mΩ·cm^2 grown by MIST EPITAXY® *Appl. Phys. Express* **9** 2–5

[81] Yang J, Ren F, Pearton S J and Kuramata A 2018 Vertical geometry, 2-A forward current Ga_2O_3 Schottky rectifiers on bulk Ga_2O_3 substrates *IEEE Trans. Electron Devices* **65** 2790–6

[82] Yang J, Ahn S, Ren F, Pearton S J, Jang S, Kim J and Kuramata A 2017 High reverse breakdown voltage Schottky rectifiers without edge termination on Ga_2O_3 *Appl. Phys. Lett.* **110** 192101

[83] Zhou H *et al* 2019 High-performance vertical β-Ga_2O_3 Schottky barrier diode with implanted edge termination *IEEE Electron Device Lett.* **40** 1788–91

[84] Lin C-H *et al* 2019 Vertical Ga_2O_3 Schottky barrier diodes with guard ring formed by nitrogen-ion implantation *IEEE Electron Device Lett.* **40** 1487–90

[85] Gao Y *et al* 2019 High-voltage β-Ga_2O_3 Schottky diode with argon-implanted edge termination *Nanoscale Res. Lett.* **14** 8

[86] Lu X, Zhang X, Jiang H, Zou X, Lau K M and Wang G 2020 Vertical β-Ga_2O_3 Schottky barrier diodes with enhanced breakdown voltage and high switching performance *Phys. Status Solidi* a **217** 3–7

[87] Hu Z *et al* 2020 Beveled fluoride plasma treatment for vertical β-Ga_2O_3 Schottky barrier diode with high reverse blocking voltage and low turn-on voltage *IEEE Electron Device Lett.* **41** 441–4

[88] Wang Y *et al* 2020 Barrier diode with thermally-oxidized termination *IEEE Electron Device Lett.* **41** 131–4

[89] Dong P, Zhang J, Yan Q, Liu Z, Ma P, Zhou H and Hao Y 2022 6 kV/3.4 mΩcm^2 vertical β-Ga_2O_3 Schottky barrier diode with $BV^2/R_{on,sp}$ performance exceeding 1-D unipolar limit of GaN and SiC *IEEE Electron Device Lett.* **43** 765–8

[90] Zhang Y, Zhang J, Feng Z, Hu Z, Chen J, Dang K, Yan Q, Dong P, Zhou H and Hao Y 2020 Impact of implanted edge termination on vertical β-Ga_2O_3 Schottky barrier diodes under OFF-state stressing *IEEE Trans. Electron Devices* **67** 3948–53

[91] Wei Y, Luo X, Wang Y, Lu J, Jiang Z, Wei J, Lv Y and Feng Z 2021 Experimental study on static and dynamic characteristics of Ga_2O_3 Schottky Barrier diodes with compound termination *IEEE Trans. Power Electron.* **36** 10976–80

[92] Karmalkar S, Shur M S, Simin G and Khan M A 2005 Field-plate engineering for HFETs *IEEE Trans. Electron Devices* **52** 2534–40

[93] Neha, Kumari V, Gupta M and Saxena M 2022 TCAD-based optimization of field plate length & passivation layer of AlGaN/GaN HEMT for higher cut-off frequency & breakdown voltage *IETE Tech. Rev.* **39** 63–71

[94] Dundar C, Kara D and Donmezer N 2020 The effects of gate-connected field plates on hotspot temperatures of AlGaN/GaN HEMTs *IEEE Trans. Electron Devices* **67** 57–62

[95] Mao W, She W B, Yang C, Zhang J F, Zheng X F, Wang C and Hao Y 2015 Reverse blocking characteristics and mechanisms in Schottky-drain AlGaN/GaN HEMT with a drain field plate and floating field plates *Chin. Phys.* B **25** 017303

[96] Tarplee M C, Madangarli V P, Zhang Q and Sudarshan T S 2001 Design rules for field plate edge termination in SiC Schottky diodes *IEEE Trans. Electron Devices* **48** 2659–64

[97] Hu S and Sheng K 2004 A new edge termination technique for SiC power devices *Solid State Electron.* **48** 1861–6

[98] Roy S, Bhattacharyya A, Ranga P, Splawn H, Leach J and Krishnamoorthy S 2021 High-k oxide field-plated vertical (001) β-Ga_2O_3 Schottky barrier diode with Baliga's figure of merit over 1 GW/cm^2 *IEEE Electron Device Lett.* **42** 1140–3

[99] Konishi K, Goto K, Murakami H, Kumagai Y, Kuramata A, Yamakoshi S and Higashiwaki M 2017 1-kV vertical Ga_2O_3 field-plated Schottky barrier diodes *Appl. Phys. Lett.* **110** 103506

[100] Green A J *et al* 2016 3.8-MV/cm breakdown strength of MOVPE-grown Sn-doped β-Ga_2O_3 MOSFETs *IEEE Electron Device Lett.* **37** 902–5

[101] Yang J, Fares C, Elhassani R, Xian M, Ren F, Pearton S J, Tadjer M and Kuramata A 2019 Reverse breakdown in large area, field-plated, vertical β-Ga_2O_3 rectifiers *ECS J. Solid State Sci. Technol.* **8** Q3159–64

[102] Yang J, Ren F, Tadjer M, Pearton S J and Kuramata A 2018 Ga_2O_3 Schottky rectifiers with 1 ampere forward current, 650 V reverse breakdown and 26.5 MW cm^{-2} figure-of-merit *AIP Adv.* **8** 055026

[103] Yang J, Ren F, Tadjer M, Pearton S J and Kuramata A 2018 2300V reverse breakdown voltage Ga_2O_3 Schottky rectifiers *ECS J. Solid State Sci. Technol.* **7** Q92–6

[104] Chen Y-T, Yang J, Ren F, Chang C-W, Lin J, Pearton S J, Tadjer M J, Kuramata A and Liao Y-T 2019 Implementation of a 900 V switching circuit for high breakdown voltage β-Ga_2O_3 Schottky diodes *ECS J. Solid State Sci. Technol.* **8** Q3229–34

[105] Allen N, Xiao M, Yan X, Sasaki K, Tadjer M J, Ma J, Zhang R, Wang H and Zhang Y 2019 Vertical Ga_2O_3 Schottky barrier diodes with small-angle beveled field plates: a Baliga's figure-of-merit of 0.6 GW/cm^2 *IEEE Electron Device Lett.* **40** 1399–402

[106] Xia X, Xian M, Carey P, Fares C, Ren F, Tadjer M, Pearton S J, Tu T Q, Goto K and Kuramata A 2021 Vertical β-Ga_2O_3 Schottky rectifiers with 750 V reverse breakdown voltage at 600 K *J. Appl. Phys.* **54** 305103

[107] Hu Z *et al* 2018 Field-plated lateral β-Ga_2O_3 Schottky barrier diode with high reverse blocking voltage of more than 3 kV and high DC power figure-of-merit of 500 MW/cm^2 *IEEE Electron Device Lett.* **39** 1564–7

[108] Liu D, Huang Y, Zhang Z, Chen D, Feng Q, You H, Zhang J, Zhang C and Hao Y 2021 Enhancing breakdown voltage of a Ga_2O_3 Schottky barrier diode with small-angle beveled and high-k oxide field plate *ECS J. Solid State Sci. Technol.* **10** 125001

[109] Li W, Saraswat D, Long Y, Nomoto K, Jena D and Xing H G 2020 Near-ideal reverse leakage current and practical maximum electric field in β-Ga_2O_3 Schottky barrier diodes *Appl. Phys. Lett.* **116** 192101

[110] Moule T, Dalcanale S, Kumar A S, Uren M J, Li W, Nomoto K, Jena D, Xing H G and Kuball M 2022

Breakdown mechanisms in β-Ga_2O_3 trench-MOS Schottky-barrier diodes *IEEE Trans. Electron Devices* **69** 75–81
[111] Li W, Nomoto K, Hu Z, Jena D and Xing H G 2020 Guiding principles for trench schottky barrier diodes based on ultrawide bandgap semiconductors: a case study in Ga_2O_3 *IEEE Trans. Electron Devices* **67** 3938–47
[112] Mechrotra M and Baliga B J 1993 The trench MOS barrier schottky (TMBS) rectifier *Proc. of IEEE International Electron Devices Meeting* (*Washington, DC, USA*) pp 675–8
[113] Li W, Nomoto K, Pilla M, Pan M, Gao X, Jena D and Xing H G 2017 Design and realization of GaN trench junction-barrier-Schottky-diodes *IEEE Trans. Electron Devices* **64** 1635–41
[114] Khemka V, Ananthan V and Chow T P 2000 Fully planarized 4H-SiC trench MOS barrier Schottky (TMBS) rectifier *IEEE Electron Device Lett.* **21** 286–8
[115] Sasaki K, Wakimoto D, Thieu Q T, Koishikawa Y, Kuramata A, Higashiwaki M and Yamakoshi S 2017 First demonstration of Ga_2O_3 trench MOS-type Schottky barrier diodes *IEEE Electron Device Lett.* **38** 783–5
[116] Takatsuka A *et al* 2018 Fast recovery performance of β-Ga_2O_3 trench MOS Schottky barrier diodes *2018 76th Device Research Conf. (DRC)* (*Santa Barbara, CA, USA, 24–27 June 2018*) pp 1–2
[117] Li W, Nomoto K, Hu Z, Tanen N, Sasaki K, Kuramata A, Jena D and Xing H G 2018 1.5 kV vertical Ga_2O_3 trench-MIS Schottky barrier diodes *2018 76th Device Research Conf. (DRC)* pp 1–2
[118] Li W, Hu Z, Nomoto K, Zhang Z, Hsu J Y, Thieu Q T, Sasaki K, Kuramata A, Jena D and Xing H G 2018 1230 V β-Ga_2O_3 trench Schottky barrier diodes with an ultra-low leakage current of <1 μA/cm^2 *Appl. Phys. Lett.* **113** 2–7
[119] Li W, Hu Z, Nomoto K, Jinno R, Zhang Z, Tu T Q, Sasaki K, Kuramata A, Jena D and Xing H G 2019 2.44 kV Ga_2O_3 vertical trench Schottky barrier diodes with very low reverse leakage current *2018 IEEE Electron Devices Meet. (IEDM)* pp 8.5.1–4
[120] Huang X, Liao F, Li L, Liang X, Liu Q, Zhang C and Hu X 2020 3.4 kV breakdown voltage Ga_2O_3 trench Schottky diode with optimized trench corner radius *ECS J. Solid State Sci. Technol.* **9** 045012
[121] Li W, Nomoto K, Hu Z, Jena D and Xing H G 2019 Field-plated Ga_2O_3 trench Schottky barrier diodes with a record-high figure-of-merit of 0.78 GW/cm^2 *2019 Device Research Conf. (DRC)* pp 209–10
[122] Li W, Nomoto K, Hu Z, Jena D and Xing H G 2020 Field-plated Ga_2O_3 trench Schottky barrier diodes with a $BV^2/R_{on,sp}$ of up to 0.95 GW/cm^2 *IEEE Electron Device Lett.* **41** 107–10
[123] Kumar S, Murakami H, Kumagai Y and Higashiwaki M 2022 Vertical β-Ga_2O_3 Schottky barrier diodes with trench staircase field plate *Appl. Phys. Express* **15** 054001
[124] Li W, Nomoto K, Hu Z, Jena D and Xing H G 2019 Fin-channel orientation dependence of forward conduction in kV-class Ga_2O_3 trench Schottky barrier diodes *Appl. Phys. Express* **12** 61007
[125] Kokubun Y, Kubo S and Nakagomi S 2016 All-oxide p-n heterojunction diodes comprising p-type NiO and n-type β-Ga_2O_3 *Appl. Phys. Express* **9** 091101
[126] Zhi Y S, Li P G, Wang P C, Guo D Y, An Y H, Wu Z P, Chu X L, Shen J Q, Tang W H and Li C R 2016 Reversible transition between bipolar and unipolar resistive switching in Cu_2O/Ga_2O_3 binary oxide stacked layer *AIP Adv.* **6** 015215
[127] Watahiki T, Yuda Y, Furukawa A, Yamamuka M, Takiguchi Y and Miyajima S 2017 Heterojunction p-Cu_2O/n-Ga_2O_3 diode with high breakdown voltage *Appl. Phys. Lett.* **111** 222104
[128] Lu X, Zhou X, Jiang H, Ng K W, Chen Z, Pei Y and Wang G 2020 1-kV sputtered p-NiO/n-Ga_2O_3 heterojunction diodes with an ultra-low leakage current below 1 μA/cm^2 *IEEE Electron Device Lett.* **41** 449–52
[129] Gong H H, Chen X H, Xu Y, Ren F F, Gu S L and Ye J D 2020 A 1.86-kV double-layered NiO/β-Ga_2O_3 vertical p-n heterojunction diode *Appl. Phys. Lett.* **117** 022104
[130] Gong H *et al* 2021 1.37 kV/12 A NiO/β-Ga_2O_3 heterojunction diode with nanosecond reverse recovery and rugged surge-current capability *IEEE Trans. Power Electron.* **36** 12213–7
[131] Hao W, He Q, Zhou K, Xu G, Xiong W, Zhou X, Jian G, Chen C, Zhao X and Long S 2021 Low defect density and small *I-V* curve hysteresis in NiO/β-Ga_2O_3 p–n diode with a high PFOM of 0.65 GW/cm^2 *Appl. Phys. Lett.* **118** 043501
[132] Lv Y *et al* 2021 Demonstration of β-Ga_2O_3 junction barrier Schottky diodes with a Baliga's figure of merit of 0.85 GW/cm^2 or a 5 A/700 V handling capabilities *IEEE Trans. Power Electron.* **36** 6179–82
[133] Gong H H *et al* 2021 β-Ga_2O_3 vertical heterojunction barrier Schottky diodes terminated with p-NiO field limiting rings *Appl. Phys. Lett.* **118** 202102
[134] Wang Y *et al* 2022 2.41 kV vertical P-NiO/n-Ga_2O_3 heterojunction diodes with a record Baliga's figure-of-merit of 5.18 GW cm^{-2} *IEEE Trans. Power Electron.* **37** 3743–6
[135] Víllora E G, Shimamura K, Kitamura K, Aoki K and Ujiie T 2007 Epitaxial relationship between wurtzite GaN and β-Ga_2O_3 *Appl. Phys. Lett.* **90** 234103
[136] Nandi A, Rana K S and Bag A 2021 Design and analysis of P-GaN/N-Ga_2O_3 based junction barrier Schottky diodes *IEEE Trans. Electron Devices* **68** 6052–8
[137] Zhou H and Ye P D T 2017 Depletion/enhancement-mode β-Ga_2O_3 on insulator field-effect transistors with drain currents exceeding 1.5/1.0 A/mm *2017 75th Annual Device Research Conf. (DRC)* pp 1–2
[138] Noh J, Si M, Zhou H, Tadjer M J and Ye P D 2018 The impact of substrates on the performance of top-gateβ-Ga_2O_3 field-effect transistors: record-high drain current of 980 mA/mm on Diamond *2018 76th Device Research Conf. (DRC)* pp 1–2
[139] Zhou H, Maize K, Noh J, Shakouri A and Ye P D 2017 Thermodynamic studies of β-Ga_2O_3 nanomembrane field-effect transistors on a sapphire substrate *ACS Omega* **2** 7723–9
[140] Zhou H, Maize K, Qiu G, Shakouri A and Ye P D 2017 β-Ga_2O_3 on insulator field-effect transistors with drain currents exceeding 1.5 A/mm and their self-heating effect *Appl. Phys. Lett.* **111** 092102
[141] Wang Y B *et al* 2020 β-Ga_2O_3 MOSFETs on the Si substrate fabricated by the ion-cutting process *Sci. China Phys. Mech. Astron.* **63** 277311
[142] Shen Z, Xu W, Xu Y, Huang H, Lin J, You T, Ye J and Ou X 2021 The effect of oxygen annealing on characteristics of β-Ga_2O_3 solar-blind photodetectors on SiC substrate by ion-cutting process *J. Alloys Compd.* **889** 161743
[143] Cheng Z *et al* 2020 Thermal transport across ion-cut monocrystalline β-Ga_2O_3 thin films and bonded β-Ga_2O_3-SiC interfaces *ACS Appl. Mater. Interfaces* **12** 44943–51
[144] Xu W *et al* 2022 Thermodynamics of ion-cutting of β-Ga_2O_3 and wafer-scale heterogeneous integration of a β-Ga_2O_3

thin film onto a highly thermal conductive SiC substrate *ACS Appl. Electron. Mater.* **4** 494–502
[145] Xu W *et al* 2019 First demonstration of waferscale heterogeneous integration of Ga_2O_3 MOSFETs on SiC and Si substrates by ion-cutting process *2019 IEEE Int. Electron Devices Meeting (IEDM)* pp 12.5.1–4
[146] Xiao M *et al* 2021 Packaged Ga_2O_3 Schottky rectifiers with over 60-A surge current capability *IEEE Trans. Power Electron.* **36** 8565–9
[147] Wang B, Xiao M, Knoll J, Buttay C, Sasaki K, Lu G Q, Dimarino C and Zhang Y 2021 Low thermal resistance (0.5 K/W) Ga_2O_3 Schottky rectifiers with double-side packaging *IEEE Electron Device Lett.* **42** 1132–5
[148] De Santi C *et al* 2019 Stability and degradation of isolation and surface in Ga_2O_3 devices *Microelectron. Reliab.* **100–101** 113453
[149] Islam Z, Xian M, Haque A, Ren F, Tadjer M, Glavin N and Pearton S 2020 *In situ* observation of β-Ga_2O_3 Schottky diode failure under forward biasing condition *IEEE Trans. Electron Devices* **67** 3056–61
[150] Zhou F *et al* 2022 1.95-kV beveled-mesa NiO/β-Ga_2O_3 heterojunction diode with 98.5% conversion efficiency and over million-times overvoltage ruggedness *IEEE Trans. Power Electron.* **37** 1223–7